2020-03-15

Numerical Investigation of the Dynamic Response of Pile Embedded in Sandy Soil Subjected to Vertical Dynamic load

Gebeyehu, Getahun

BAHIR DAR UNIVERSITY

BAHIR DAR INSTITUTE OF TECHNOLOGY

SCHOOL OF RESEARCH AND POSTGRADUATE STUDIES

FACULTY OF CIVIL AND WATER RESOURCE ENGINEERING

Numerical Investigation of the Dynamic Response of Pile Embedded in Sandy Soil Subjected to Vertical Dynamic Load

Getahun Gebeyehu

Bahir Dar, Ethiopia

August 1,2019

Numerical Investigation of the Dynamic Response of Pile Embedded in Sandy Soil Subjected to Vertical Dynamic load

Getahun Gebeyehu Gezahegn

A Thesis Submitted to The School of Research and Graduate Studies of Bahir Dar Institute of Technology, BDU in partial fulfillment of the requirements for the degree of

Masters in Civil Engineering (Geotechnical Engineering major) in the Faculty of civil and Water Resource Engineering.

Advisor: Dr.Tensay Geberemedhin

Bahir Dar, Ethiopia

August 1,2019

DECLARATION

I, the undersigned, declare that the thesis comprises my own work. In compliance with internationally accepted practices, I have acknowledged and refereed all materials used in this work. I understand that non-adherence to the principles of academic honesty and integrity, misrepresentation/fabrication of any idea/data/fact/source will constitute sufficient ground for disciplinary action by the University and can also evoke penal action from the sources which have not been properly cited or acknowledged.

Name of the student Getahun Gebeyehu Signature _____

Date of submission: _____

Place: Bahir Dar

This thesis has been submitted for examination with my approval as a university advisor.

Advisor Name: Dr. Tensay Geberemedhin .

Advisor's Signature: _____

Babir Dar Institute of Technology-

School of Research and Graduate Studies

Faculty of Civil and Water Resource Engineering

THESIS APPROVAL SHEET

Student:

Getahun Gebeyehu		August 9/2019
Name	Signature	Date

The following graduate faculty members certify that this student has successfully presented the necessary written final thesis and oral presentation for partial fulfillment of the thesis requirements for the Degree of Master of Science in Civil Engineering (Geotechnical Engineering major)

Approved By:

Advisor:

Dr. Tensay Geberemedhin		11/07/19
Name	Signature	Date

External Examiner:

Dr.-Ing. Henok Fikire		08/08/2019
Name	Signature	Date

Internal Examiner:

Dr. Sirai Mulugeta		16/08/2019
Name	Signature	Date

Chair Holder:

Mr. Wubetie Mengist		29/08/2019
Name	Signature	Date

Faculty Dean:

Dr. Temesegen Enku		Aug. 29, 2019
Name		Date

Temesegen Enku Nigussie (PhD)
Faculty Dean

To my father and mother

ACKNOWLEDGEMENTS

While doing this thesis, many made considerable contributions for which I would like to extend heartfelt thanks. Above all, I should forever glorify the Almighty God who holds my life and all my ways in his hands and for the indescribable and unconditional love and help in each and every aspect of my life.

I want to also extend my deepest gratitude to Bahir dar Institute of Technology in collaboration with my home university, Debre Tabor University, for giving me a full scholarship. Without this my study might not have been possible as getting education without sponsorship is becoming very difficult right today.

Next, I have found that it is an honor for me to thank my instructor and advisor Dr.Tensay Geberemedhin, Senior Scientist of Geotechnical Engineering, for his unmeasurable contribution starting from developing the proposal to end of the thesis work. Especially, his extraordinary readiness and capability of guiding on Finite difference software called FLAC^{3D} was unforgettable. Frankly speaking, it is a big privilege to have such a whole rounded experts as a course lecturer and as an advisor in a research in order to accomplish meaningful works and hit the goal, and I fell as if I am lucky of getting him as my advisor.

My appreciation and thank also goes to my instructor Dr. Addiszemen Teklay for his relentless devotion to give me his mount expertise, knowledge and materials in the area of advanced foundation engineering which have supported me in carrying out the thesis.

I would like to also thank my classmates and friends on their uncontrolled help while doing this research and especially I am thank full of my junior students on lending me their personal computers while I was modeling my task in FLAC^{3D}.

Last, but by no means least, special thanks to my family and relatives for their relentless support and encouragement throughout the study period is extended.

Getahun Gebeyehu

Bahir Dar, Ethiopia, 2019

ABSTRACT

The interaction of the soil with the structure has been largely explored with the assumption of material and geometrical linearity of the soil. Nevertheless, for moderate or strong seismic events, the maximum shear strain can easily reach the elastic limit of the soil behavior. Hence the nonlinear effects may change the soil stiffness energy dissipation into the soil. Consequently, ignoring the nonlinear characteristics of the dynamic soil-structure interaction could lead to erroneous predictions of structural and/or geotechnical response.

The goal of this work, therefore, is to implement a fully nonlinear constitutive model for soils into a numerical code through Sigmoidal 4 non-linear constitutive model in order to investigate the effect of soil nonlinearity on dynamic soil pile interaction using the finite difference software called FLAC^{3D}. The implemented model was first numerically verified by comparing the results with what is done laboratorically for the same soil properties. Afterward, a parametric study was carried out for different frequency variation in such a way that some extensions were made just beyond the fundamental frequency after determining it to characterize nonlinear effects.

Different features of the dynamic soil-pile interaction were investigated after wards: the variation of settlement of the pile head with frequency, the characteristics of pile deformation with the pile length, the distribution of axial force with frequency, the variation of skin friction with frequency, the Characterstics of axial force distribution with the pile length and that of skin friction with pile length was investigated. It was shown that a point where the fundamental frequency of the structure and the natural frequency of the soil were coincided simultaneously, the response of the pile was found to be maximum and it was also the point where direction of increment was changed. Also the Characterstics of axial force distribution and skin friction were reversed to each other with frequency.

KEY WORDS: nonlinear soil, dynamic soil-pile interaction, FLAC^{3D}, Sigmoidal 4, soil-pile interface

TABLES OF CONTENT

LIST OF ABBREVATIONS

FE	Finite element
FD	Finite Difference
FEM	Finite element Method
FDM	Finite Difference Method
FDP	Finite Difference Programs
SSI	Soil structure Interaction
2D	Two Dimension
3D	Three Dimension
PSS	Pile Soil system
FLAC ^{3D}	Fast Lagrangian Analysis of Continua in 3 Dimension
GIIC	Graphical Interface for Itasca Codes
DSSI	Dynamic soil structure interaction
DLL	Dynamic Link Library
cs scoh	shear coupling spring cohesion per unit length, *cs* [F/L]
cs sfric	shear coupling spring friction angle [degrees]
cs sk	shear coupling spring stiffness per unit length [F/L2]
cs ncoh	Normal coupling spring cohesion per unit length [F/L]
cs nfric	Normal coupling spring friction angle [degrees]
cs nk	Normal coupling spring stiffness per unit length [F/L^2]
Xcarea	Cross-sectional area, *A* [L2]
Xciy	Second moment with respect to pileSEL *y*-axis, *Iy* [L^4]
Xciz	**S**econd moment with respect to pileSEL *z*-axis, *Iz* [L^4]
Xcj	Polar moment of inertia, *J* [L^4]
Emod	Young's modulus, *E* [F/L^2]
Nu	Poisson's ratio, *v*
pileSEL	Pile structural element
His	history point
Szz	stress in the Z direction
Xdis	displacement (deformation) in the x-direction

Ydis	displacement (deformation) in the y-direction
Zdis	displacement (deformation) in the z-direction
Xv	velocity in the x- direction
Yv	velocity in the y- direction
Zv	velocity in z- direction
cs ngap	Normal coupling spring gap-use flag, g

LIST OF SYMBOLS

C	Damping Matrix
E	elastic Modulus
G	Shear Modulus
Q	Complex harmonic load
Q	Input Value of the load
K	Stiffness Matrix
C_z	Equivalent viscous Damping
K_1	Real stiffness matrix
Z	Displacement
$\dot{Z}$	Velocity
$\ddot{Z}$	Acceleration
f	Frequency
γ	Unit Weight
ν	Poisons Ratio
ε	Strain
Φ	internal Friction Angle of the soil
ω	Angular frequency
λ	Wave length
Δl	The spatial element size
ρ	Mass density
σ_n	Applied normal stress
σ_s	Applied shear stress
Cs	speed of S-wave propagation through media
C_p	Speed of p-wave propagation through media
M_s	Secant modulus
Φo	Initial phase angle
X, Y	Amplitude multipliers

LIST OF FIGURES

LIST OF TABLES

1. INTRODUCTION

Geotechnical analysis is determining of internal stress resultants (axial, bending and shear) and strain resultant (rotation and displacement) of a structure under a given geometric data and materials property. Most of the time, Geotechnical analysis is done before Geotechnical design and, therefore, the accuracy of analysis is fundamental for good product. The analysis methods are of the type linear or nonlinear (CSI, 2009).

Linear Analysis (Small Strain) Method

- Linear force displacement relationship(i.e., Hooke's Law):$[K]\{x\} = \{F\}$
- Because [K] is assumed to be constant, essentially only linear behavior is allowed.
- In many real-world situations, however, this small-displacement theory may not be valid. In such situations, nonlinear analysis is required.

The linear equilibrium equations are independent of the applied load and the resulting deflection (CSI, 2009). Thus the results of different static and/or dynamic loads can be superposed (scaled and added), resulting in great computational efficiency. If the load on the structure and/or the resulting deflections are large, then the load-deflection behavior may become nonlinear (Hardin and Drench, 1985).

Once a nonlinear analysis has been performed, its final stiffness matrix can be used for subsequent linear analyses (CSI, 2009). Any geometric nonlinearity considered in the nonlinear analysis will affect the linear results.

Several causes of this nonlinear behavior can be identified (CSI, 2009) :

- **Large-displacement effect:** when soil under goes large deformation (in particular, large strains and rotations), the usual engineering stress and strain measures no longer apply, and the equilibrium equations must be written for the deformed geometry. This is true even if the stresses are small.

- **Material nonlinearity:** when a material (soil) is strained beyond its proportional limit, the stress-strain relationship is no longer linear. Plastic materials strained beyond the yield point may exhibit history dependent behavior. Material nonlinearity may affect the load-deflection behavior of a structure even when the equilibrium equations for the original geometry are still valid.
- **Other effects:** Other sources of nonlinearity are also possible, including non -linear loads, boundary conditions and constraints.

Nonlinear analysis solutions require several iterations (ANSYS, 2005). The actual relationship between load and displacement is not known beforehand, and consequently a series of linear approximations with corrections is performed. This is a simplified explanation of the Newton-Raphson method (shown as solid lines in figure1.1).In the Newton-Raphson Method, the total load F_a is applied in iteration 1. The result is x_1. From the displacements, the internal forces F_1 can be calculated. If $F_a \neq F_1$, then the system is not in equilibrium. Hence, a new stiffness matrix is calculated based on the current conditions. The difference of F_a - F_1 is the out-of-balance or residual forces. The residual forces must be 'small' enough for the solution to converge. This process is repeated until $F_a = F_i$. In this example, after iteration 4, the system achieves equilibrium and the solution is said to be converged.

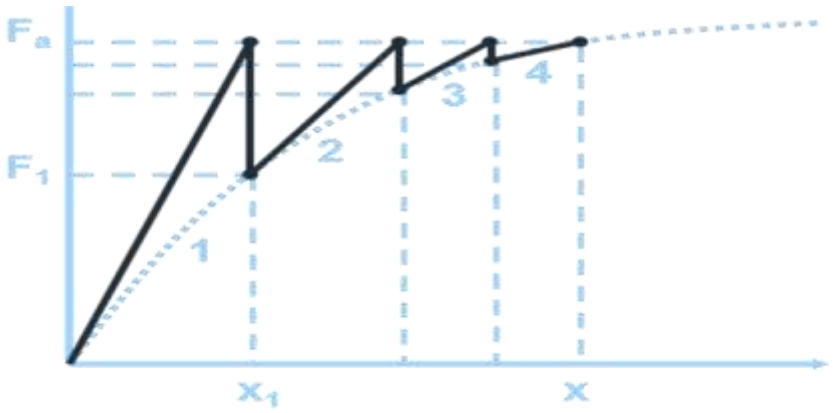

Figure 1.1 Newton Raphson method for nonlinear structural analysis (ANSYS, 2005)

1.1. Introduction to Dynamics of Soil pile System

The assessment of dynamic soil-structure interaction needs several parameters to be identified: site geometry, the nonlinear soil behavior under cyclic loading, the soil material properties, the dynamic response of the superstructure, the wave content and amplitude modifications due to stiffness of the structures. Nevertheless, due to the limitation of the state of the art of the today's numerical method, several simplifications must be done in order to formulate a soil-pile interaction problem. In this section, a global definition of the dynamic soil pile interaction problem is presented.

For low-speed machineries subjected to vertical vibration, the natural frequency of the foundation-soil system should be at least twice the operating frequency. In the design of these types of foundations, if changes in size and mass of the foundation (more popularly known as tuning of a foundation) do not lead to a satisfactory design, a pile foundation may be considered. It is also possible that the subsoil conditions are such that the vibration of a shallow machine foundation may lead to undesirable settlement. In many circumstances the load-bearing capacity of the soil may be low compared to the static and dynamic load imposed by the machine and the shallow foundation. In that case the design will then dictate consideration of the use of piles. It should be kept in mind that the use of piles will, in general, increase the natural frequency of the soil–pile system and may also increase the amplitude of vibration at resonance. The soil structure interaction of the deep foundations is not well understood and though rigorous theoretical solutions exist, they are mostly confined to researchers than designers. The practice in design offices is usually based on ignoring the stiffness of the soil and only the stiffness of the pile is taken into account. In this research, the fundamental concepts of pile foundations subjected to vibrating loads will be considered. It should also be kept in mind that the piles supporting machine foundation are for cases of low amplitudes of vibration (because allowable motion is small and dynamic loads are small compared to static loads) in contrast to those encountered under earthquake-type loading.

A pile experiencing dynamic load under a major earthquake is actually probabilistic. It may or may not happen in the life span of a structure, as because return period of an earthquake

is usually 1 in 50 years. However, for foundations subjected to vibrational loads as in machine foundation, foundations of Stadiums and the like supported on piles, this is an absolute certainty and to researchers perception a serious knowledge gap still exists.

1.2. Background of the study

Pile foundation is part of structure that is used to transfer the loads of the structure to a deeper soil or rock with a higher bearing capacity, avoiding the shallow soil with low bearing capacity. Piles are commonly used as foundations of tall buildings, bridge, dams, transmission towers, earth retaining structures, and etc. In most situations, the primary function of pile foundation is to transfer the axial loads arising from the weight of super structures. Even though the primary function is to transmit axial loads in most cases, every pile foundation has to with stand some lateral loads.

When the piles are loaded axially, part of the load is transferred to the ground through the base of the pile as base resistance and part is transferred through the pile shaft as shaft or skin friction (Figure 1.2a). If the resistive force exceeds the limit, pile may fail causing an excessive deflection. Laterally loaded piles, on the other hand, transfers the load to the surrounding soil mass through the lateral resistance of soil. When lateral loads are applied on the pile, the pile tries to shift in the direction of the applied load, pressing against the soil in front of the pile (Figure1.3b) which will generate compressive and shear stress and strains in the soil. The total soil resistance acting across the pile shaft balances the external lateral forces

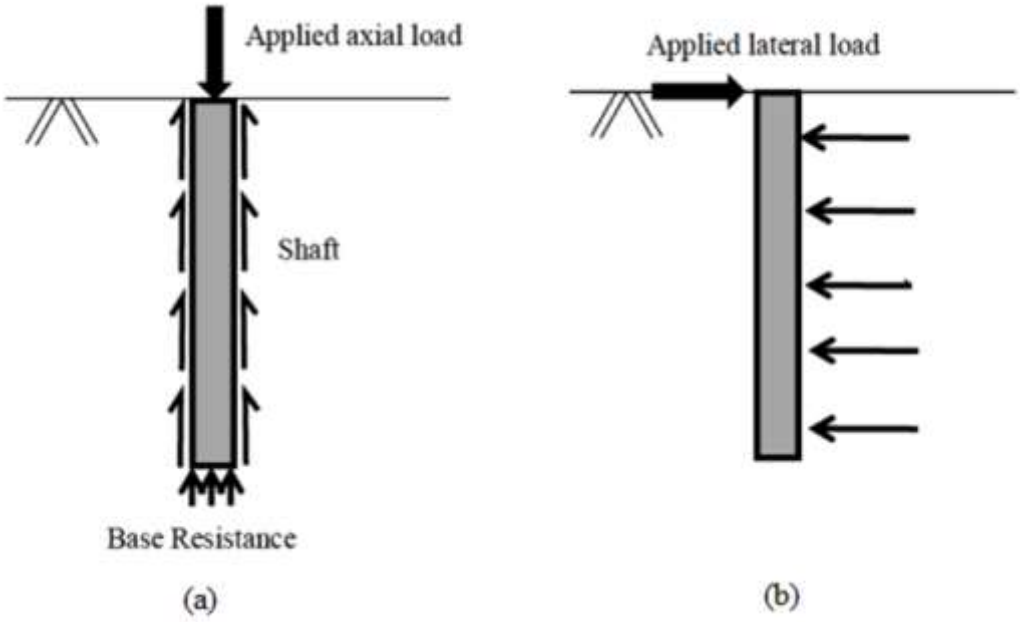

Figure 1.2 Load transfer mechanism in pile foundations after (Bowles, 1996)

1.3. Problem Statement

Usually in the seismic design of ordinary building, soil structure interaction is neglected and the dynamic response of the structure is evaluated under the assumption of a fixed based response. However, during seismic loading the soil undergoes deformations which are imposed to the foundation. In previous studies there was tremendous effort to improve the quality of linear analysis for dynamic behavior of the materials to be used in the construction of particular civil structures. Building codes, on the other hand, have been modified to cope up with the state of the art analysis methods, the way of changing the dynamic load to equivalent static load and designing the civil structure is preceded in the code called Ethiopian Building code Standards (EBCS, 2013). However, in the code there is no visible effort to come with the effect of the dynamic load on soil structure interaction without changing it to Equivalent static load. Hence, this research tries to answers this gap.

1.4. Objective of the study

General objective:

This thesis is mainly targeted to determine the dynamic response of an interacting soil-pile foundation with respect to settlement of the pile by varying the variation of loading frequency.

Specific objectives: These are some of the specific objectives of this research

- To recommend for the designers to take care of while designing dynamically loaded structures.
- To investigate the behaviour of friction stress and axial load distribution as a result of dynamic load on soil-pile foundation system.
- To show the clear difference between the linear and nonlinear response of pile foundations for vertical dynamic load such a way that linear response of pile foundations have been investigated in previous researchers.

1.5. Significance of the study

Most foundations have been designed considering that as if they are subjected to static loads due to the fact that static loads are greater in magnitude than that of dynamic load and the duration of loading also varies while both loading conditions are applied simultaneously, which is principle of relativity, so that the dynamic response of pile have been given less credit. Basically, this research tried to give insight about the effect of dynamic load on civil structures analysis. It also tries to insist Civil engineers of the current time, to be familiar with designing of structures subjected to dynamic load if the output of this research reveals that the effect of dynamic response is significant and the software's will give the same result.

2. LITERATURE REVIEW

2.1 General

In this chapter an extensive literature review of soil piles interaction behavior subjected to dynamic loading was made. Researching on behavior of pile subjected to vertical vibration loading in different soil type has been a challenge for geotechnical engineers for the last long years. The majority of these researches dealt with the static loadings and dependent on laboratory and field test determination of the response of piles on such loadings. In this research, therefore, was going to consider the response of pile structure subjected to dynamic loading using numerical methods of investigation. The behavior of single pile under axial static loading was examined in detail by many investigators, and their findings were outlined in several publications (Fekadu, 2010), (Mamo, 2016.), and etc. The behavior of pile subjected to vertical dynamic load, however, is more complex and has not been adequately examined or understood while many model tests were carried out (Adimoolam et al, 2013), (Ali Gandomzadeh etal, 2008).

2.2 A Brief History on Development of Dynamic Response of Piles

Behavior of pile foundations even under static load is quite complex. And a number of empirical factors get plugged in to the basic equilibrium equation to ensure that theoretical computations match with field observed data. This might have prompted by Terzaghi K to state that "…….theoretical refinements in dealing with pile problems are completely out of place and can be safely ignored''. The statement did not possibly bodeominous, where protagonists of the Terzaghian School often scoffed at attempt of any theoretical development in area of pile dynamics. And this was a serious stunted progress in that difficult time in the area of soil dynamics. Fortunately, not everybody around the world got discouraged by this pessimistic assessment and a number of analytical and numerical approaches to analysis of pile dynamic behavior have been developed, that has far superior theoretical basis for pile design than the equivalent cantilever concept or other purely empirical methods that dominated the field (Nogami et al, 1991).

Many sophisticated linear and nonlinear models were proposed to study the lateral response of piles under dynamic loads (Gandomzadeh, 2011), (Mohammad M . Ahmedin and Mahdi Ehsan, 2008), but there are only a very few full scale experimental data available to confirm the reliability of these models. The major full-scale field testing carried out on piles embedded in clay and sandy clay sites by various authors (Boominathan A. and Ayothiraman R., 2006) clearly demonstrate that the performance of existing linear and nonlinear models are highly dependent on in-situ soil nonlinearity and dynamic loading characteristics. Hence, conducting in-situ full-scale dynamic tests on piles in order to have a better understanding of nonlinear response of piles should accurately assess the dynamic characteristics of soil-pile system.

2.3 Dynamics of a soil-pile system

According to statically loaded pile researchers, if the long-term response of a structure to applied loads is sought, a static analysis has to be performed as the duration of loading is large and even may permanently applied throughout the life of a foundation. However, if the loading has a short duration as in the cases of machine vibrations, stadiums, compaction, pile driving, wave loading and earthquake, the loading condition is dynamic in nature. Thus, a dynamic analysis ought to be executed. Dynamic stiffness of soil including both elastic stiffness and damping can be represented by a complex quantity of the data. Thus, it needs to use a FE or FD program/s capable of running complex-harmonic analyses. In the complex data representation, the real part represents the spring stiffness and the imaginary part represents damping.

2.3.1 Pile Behavior under Dynamics

The vibrational effects of the pile foundation depends on the type of pile bearing, the type of soil through which it embedded in and the length and Weight of pile itself. Accordingly piles subjected to vertical vibration can be classified as End –bearing piles and Friction piles.

2.3.1.1 End Bearing Piles

These piles penetrate through soft soil layers up to a hard stratum or rock. The hard stratum or rock can be considered as rigid just at the tips of the piles. Figure 2.1 shows a pile driven up to a rock layer. The length of the pile is equal to *L*, and the load on the pile coming from the foundations is ***Q***. This problem can be approximately treated as a vertical rod fixed at the base (that is, at the rock layer) and free on top.

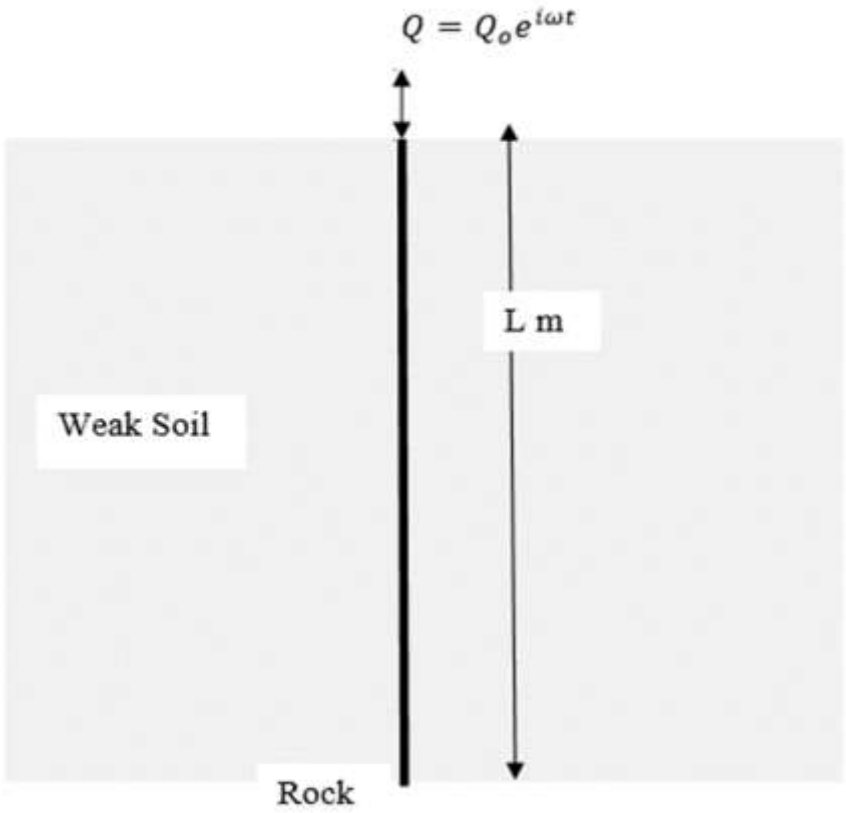

Figure 2.1 End bearing pile (Braja M. Das, G.V. Ramana, 2011)

These type of piles penetrate through soft soil layers up to a hard stratum or rock. The hard stratum or rock can be considered as rigid. For this type of piles, the natural frequency of vibration can be given by equation 2.1 (Braja M. Das, G.V. Ramana, 2011)

$$\frac{L\gamma_P}{\sigma_0} = \left(\frac{\omega_n L}{v_{c(p)}}\right) tan\left(\frac{\omega_n L}{v_{c(p)}}\right) \qquad 2.1$$

Where A = area of the cross section of the pile.

γ_P= unit weight of the pile material.

ω_n = natural circular frequency.

$v_{c(p)}$ = longitudinal wave propagation velocity in the pile.

$\sigma_0 = \frac{W}{A}$

L= length of pile (m)

Then the natural Frequency can be determined using

$$f_n = \frac{\omega_n}{2\pi} \qquad 2.2$$

2.3.1.2 Friction Piles

The tips of these piles do not rest on hard stratum. The piles resist the applied load by means of frictional resistance developed at the soil-pile interface, in which this particular research focuses on. Figure 2.2 bellow shows a pile having a length of embedment equal to *L* and a radius of *R*. The pile is subjected to a dynamic load of (Braja M. Das, G.V. Ramana, 2011)

$$Q = Q_o e^{i\omega t}$$

In this type of piles, unlike the end bearing piles, the vibrational load starts to transmit to the soil ,under which it has embedded in, just starting from the peak of the pile (at the point where the pile starts to contact with the soil).The transfer mechanism is just throughout the length of the pile shaft. Such load transferring conditions are mostly expected when pile foundations are embedded in sandy soil. Depending on the soil type, therefore, the total load may even transfer to the soil with in the length of the pile just before the pile tip. Even the length of friction piles depend on the shear strength of the soil, the applied load, and the pile size. To determine the necessary lengths of these piles, an engineer needs a good

understanding of soil pile interaction, good judgment, and experience. Hence the study of soil pile interaction is found to be studied.

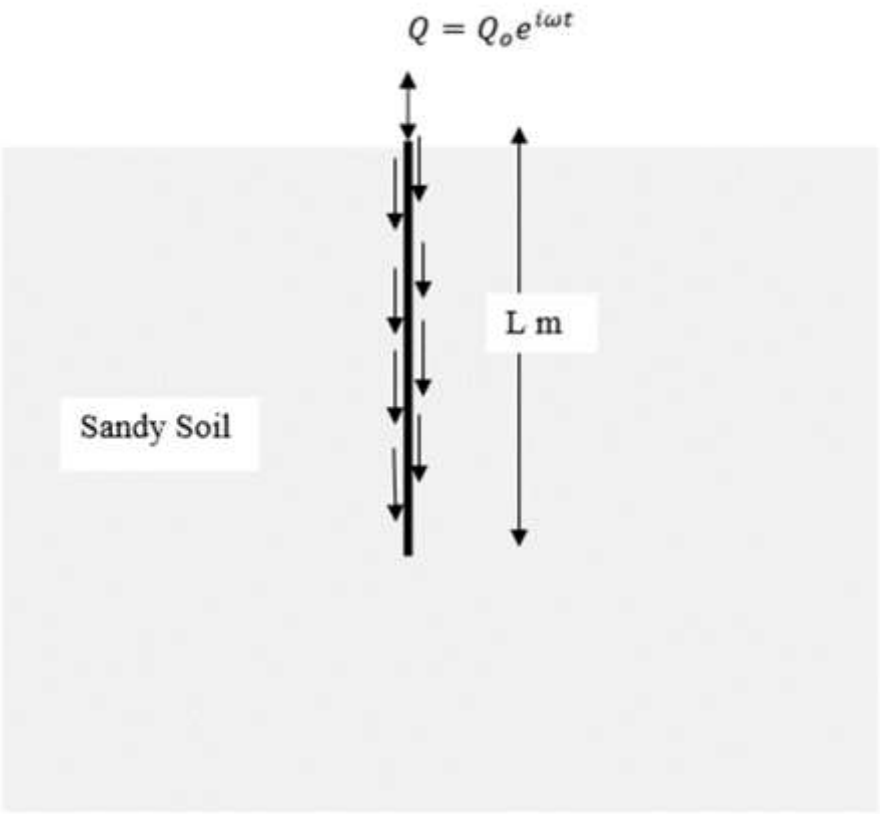

Figure 2.2 Friction piles embedded in sandy soil (Braja M. Das, G.V. Ramana, 2011)

The mathematical formulation for obtaining the stiffness (K_z)and the damping (C_z) parameters has been given by (Braja M. Das, G.V. Ramana, 2011) , While developing the empirical theory, the following assumptions were made:

1. The pile is vertical, elastic, and circular in cross section.

2. The pile is floating.

3. The pile is perfectly connected to the soil.

4. The soil above the pile tip behaves as infinitesimal, thin, independent linearly elastic layers.

The last assumption leads to the assumption of plane strain condition. The dynamic stiffness and damping of the pile can then be described in terms of complex stiffness (Braja M. Das, G.V. Ramana, 2011)as

$$k = k_1 + ik_2 \qquad 2.3$$

The applied force *Q* and displacement *z* are related to *k* in the following manner:

$$Q = k_z = (k_1 + ik_2)z \qquad 2.4$$

$$where\ i = \sqrt{-1}$$

k_1 = real part of k = Re k and k_2 = imaginary part of k = Im k

Hence, the spring constant is;

$$k_z = k_1 = \text{Re } k \qquad 2.5$$

And the equivalent viscous damping is;

$$C_z = \frac{k_2}{\omega} = \frac{Imk_2}{\omega} \qquad 2.6$$

So, the force-displacement relation can be expressed as

$$Q = K_z Z + c_z \dot{Z} \qquad 2.7$$

Where $\dot{Z} = \frac{dZ}{dt}$

The relationships for k_z and C_Z have been given by as

$$k_z = \left(\frac{E_p A}{R}\right) f_{z1} \qquad 2.8$$

And

$$C_Z = \left(\frac{E_P A}{G/\rho}\right) f_{z2} \qquad 2.9$$

Where E_P= modulus of elasticity of the pile material

A = area of pile cross section

G = shear modulus of the soil

ρ = Density of Soil

f_{z1}, f_{z2} = non dimensional parameters

The f_{z1} and f_{z2} variations for floating piles are shown in Figures 2.3 and 2.4

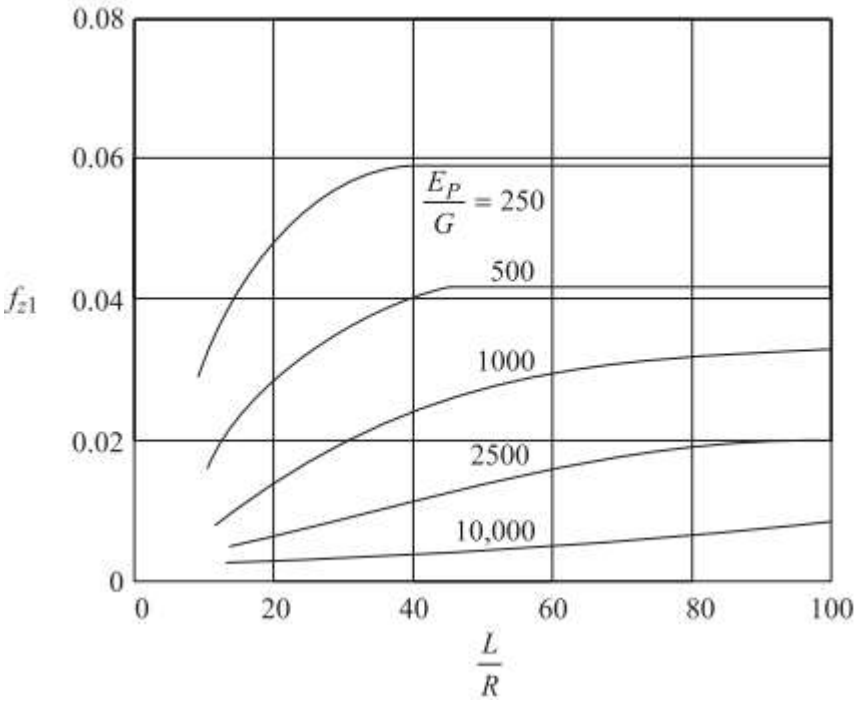

Figure 2.3 Variation of f_{z1} with $\frac{L}{R}$ and E_p/G for floating piles (Braja M. Das, G.V. Ramana, 2011)

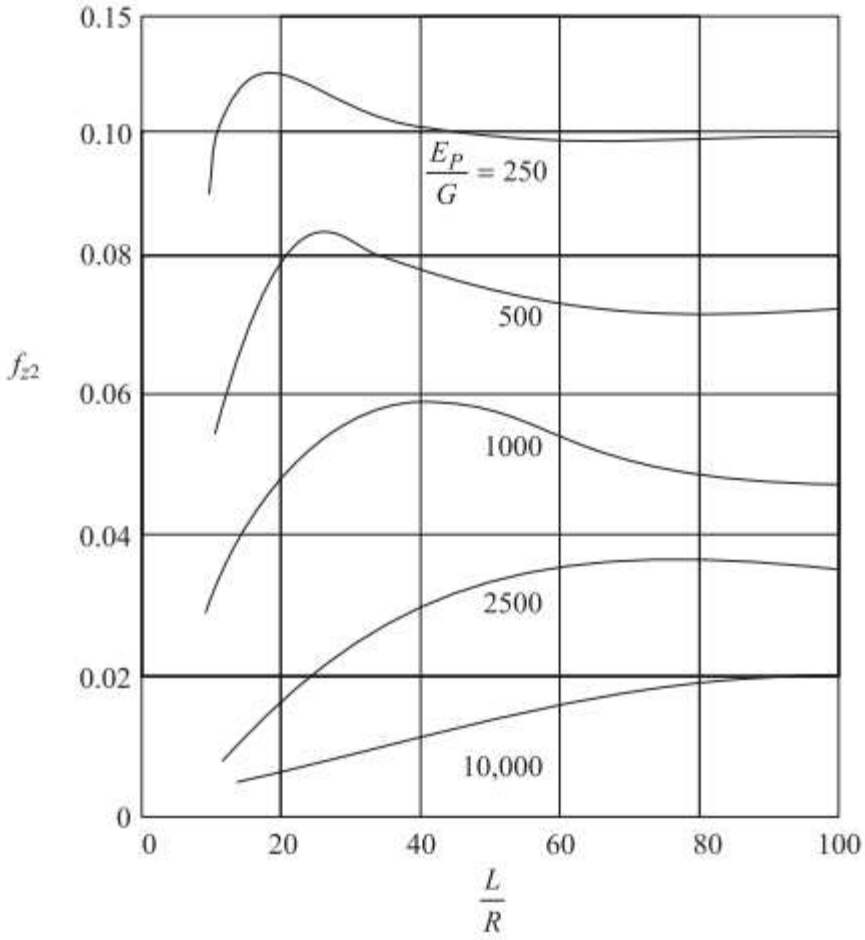

Figure 2.4 Variation of f_{z1} with $\frac{L}{R}$ and $^{E_p}/_{G}$ for floating piles after (Braja M. Das, G.V. Ramana, 2011)

Once k_z and C_Z are calculated as in equation 2.7 and 2.8, it is easy to calculate the damping ratio and natural frequency of the pile which is the resonance point.

i) The damping ratio

$$D_z = \frac{C_z}{2\sqrt{k_z m}} \qquad 2.10$$

And

ii) Undamped natural frequency of

$$\omega_n = \sqrt{\frac{k_z}{m}} \qquad 2.11$$

$$f_n = \left(\frac{1}{2\pi}\right)\sqrt{\frac{k_z}{m}} \qquad 2.12$$

Where m is the mass of the foundation and pile cap. This is so because the mas of the foundation and mass of the pile cap is maximum with relative to mas of the pile but in case of single pile since the pile cap is rejected the mass of the pile is taken as the mas of the pile cap.

iii) Damped natural frequency

$$f_m = f_n\sqrt{1 - 2{D_z}^2} \qquad 2.13$$

iv) Amplitude of vibration at resonance:

$$A_z = \frac{Q_0}{k_z}\frac{1}{2D_z\left(\sqrt{1 - {D_z}^2}\right)} \qquad 2.14$$

2.3.2 Physical Properties of Typical Sand Soil

In this sub-section it was intended to review previous works on the characterization of the physical properties of typical sand soil relevant to this work. Several manuals and studies have been published regarding on the physical properties of typical sands. Empirical correlations or values for the necessary material characteristics were employed in the present study. Since elastic and plastic properties of the pile and soil are required respectively, it was necessary to review both properties from different literatures. The young's modulus and Poisson's ratio define a given perfectly elastic material. Whereas, if one uses the Mohr-Columb plastic constitutive model, then cohesion and angle of internal friction will define the plastic behavior of a given material like soil and rocks (Gandomzadeh, 2011). In this study, therefore, the Mohr-Columb constitutive model was employed for static analysis and sigmoidal model, nonlinear dynamic model, was used to model the dynamic properties of the soil. In the subsequent sections, therefore, relevant soil

and pile material properties were reviewed from different literatures which are helpful for such conditions. Accordingly, each parameter that defines elastic and plastic behavior of soils was reviewed even those parameters were taken from a laboratory result of a research made ever.

2.3.2.1 Angle of Internal Friction

Angle of internal friction is nothing but it is an angel between shear stress and normal effective stress while these values are drawn in Mohr's Circle at which shear failure occurs or it is the maximum angle of obliquity at which sliding of unstable soil mass over a stable soil mass will occur. One of the empirical correlations of angle of internal frictions with SPT numbers for sands have been given in table 2.1 bellow.

Table 2.1 Typical angle of internal friction for sand soils after (Bowles, Joseph E., 1996)

SPT Penetration,N-Vlues(blows/foot)	Density of Sand	φ(in degrees)
3-6	Very loose	28- 30
5-9	Loose	30-34
10-25	Medium	33-40
26-45	Dense	40-50
>45	Very dense	< 50

2.3.2.2 Unit Weight

Unit weight of a soil mass is the ratio of the total weight of soil to the total volume of soil within a specified soil sample. Empirical values for unit weight, γ, of granular soils based on the standard penetration number are given in table 2.2 bellow

Table 2.2 Typical unit weight Values of granular soil after (Bowles, 1996)

SPT Penetration,N-Vlues	γ (Ib/ft^3)	γ (kN/m^3)
0-4	70-100	11-16
4-10	90-115	14-18
11-30	110-130	17-20
31-50	110-140	17-22
>50	130-150	20-22

2.3.2.3 Modulus of Elasticity (Young's Modulus)

Elastic modulus is a measure of the resistance of a material to elastic (or 'springy') deformation. If rods of identical cross-section are laid on two widely spaced supports and then identical weights are hung at their centers, they bend elastically by very different amounts depending on the material of which they are made. This is so because different materials have their own modulus of elasticity as one part of parameter. The modulus is reflected, too, in the natural frequency of vibration of a structure. A pile of low modulus has a lower natural frequency than one of higher modulus (although the density matters also) and this, as well as the deflection, is important in design calculations.

The modulus of elasticity or Young's modulus of a soil is, therefore, an elastic soil parameter most commonly used in the estimation of settlement from static loads. Young's modulus, E, may be estimated from empirical correlations, laboratory test results and field tests. The young's modulus is also used to estimate the dynamic soil property of shear modulus, which is the maximum shear modulus of the soil and starts to decrease in value while a soil is subjected to vibration with in the corresponding cyclic shear strain and hence becomes necessary soil parameter whether the soil is model linearly on in nonlinearly dynamic condition. Typical values of elastic moduli for sand soil are presented in table 2.3 bellow.

Table 2.3 Typical elastic moduli of sand soil after (Bowles, 1996)

Sandy Soil	E, kPa
Loos sand	9500-23750
Dense Sand	23750-95000

2.3.2.4 Poisson's ratio

Poisson's ratio is the negative ratio of transverse to axial strain. When a material is compressed in one direction, it usually tends to expand in the other two directions perpendicular to the direction of compression. This phenomenon is called the Poisson effect. The typical values of Poisson's ratio were taken from table 2.4 bellow.

Table 2.4 Typical Poisson's ratio of soils after (Bowles, 1996)

Soil	Poisson's Ratio
Most clay soils	0.4-0.5
Saturated clay soils	0.45-0.5
Chohesionless, medium and dense	0.2-0.35
Chohesionless, loose to medium	0.3-0.4

2.4 Soil Behavior under Dynamics

For soil sites, describing the soil configuration (layering or stratigraphy) and the dynamic material properties of soil is necessary to perform SSI analysis and predict soil structure response. The physical properties of soil studied in section 2.3.2 are going to be vulnerable to a slight change while subjected to cyclic loading which are appropriate to use in dynamic modeling of a structure embedded in soil media. Determining soil properties to be used in the SSI analysis is the second most uncertain element of the process, the first being specifying induced dynamic load. Modeling the soil, then, can be visualized in two stages:

determining the low strain in situ soil profile and associated material properties and defining the dynamic material behavior of the soil as a function of the induced strains from the earthquake (Induced dynamic load) and soil structure response (Mohammad M . Ahmedin and Mahdi Ehsan, 2008). In general, dynamic stress–strain behavior of soils is nonlinear, anisotropic, elastoplastic, and loading path dependent which are determined in fields and laboratory (Wood, 1990)

2.4.1 Field Exploration

Field exploration, typically, relies heavily on boring programs which provide information on the spatial distribution of soil (horizontally and with depth) and produce samples for laboratory analysis. In addition, some dynamic properties are measured in situ, for example, shear wave velocity which leads to a value of shear modulus at low strains. (Wood, 1990) Provides a summary of field exploration, in general, and of boring, sampling, and in-situ testing, in particular. Low strain shear and compressional wave velocities are typically measured in the field.

2.4.2 Laboratory Tests

Some aspects of dynamic soil behavior are easier to study in a laboratory, under controlled stress conditions. In addition, a comprehensive understanding of the soil behavior under cyclic loading requires the realization of numerous tests carried out under various stress conditions and load paths. These conditions can only be achieved in a laboratory. However, to be representative of the actual soil behaviour, these tests have to be performed on truly undisturbed samples, which are capable of restoring the past history of the deposit in terms of strain and stress paths. Laboratory tests are, therefore, used principally to measure dynamic soil properties and their variation with strain: soil shear modulus and material damping. Currently available laboratory testing techniques have been discussed and summarized by (Wood, 1990). Generally, the modulus reduction curves for gravelly soils and sands are similar.

Figure 2.5 shows material damping as a function of shear strain. Shear modulus decreases and material damping increases with increasing shear strain levels.

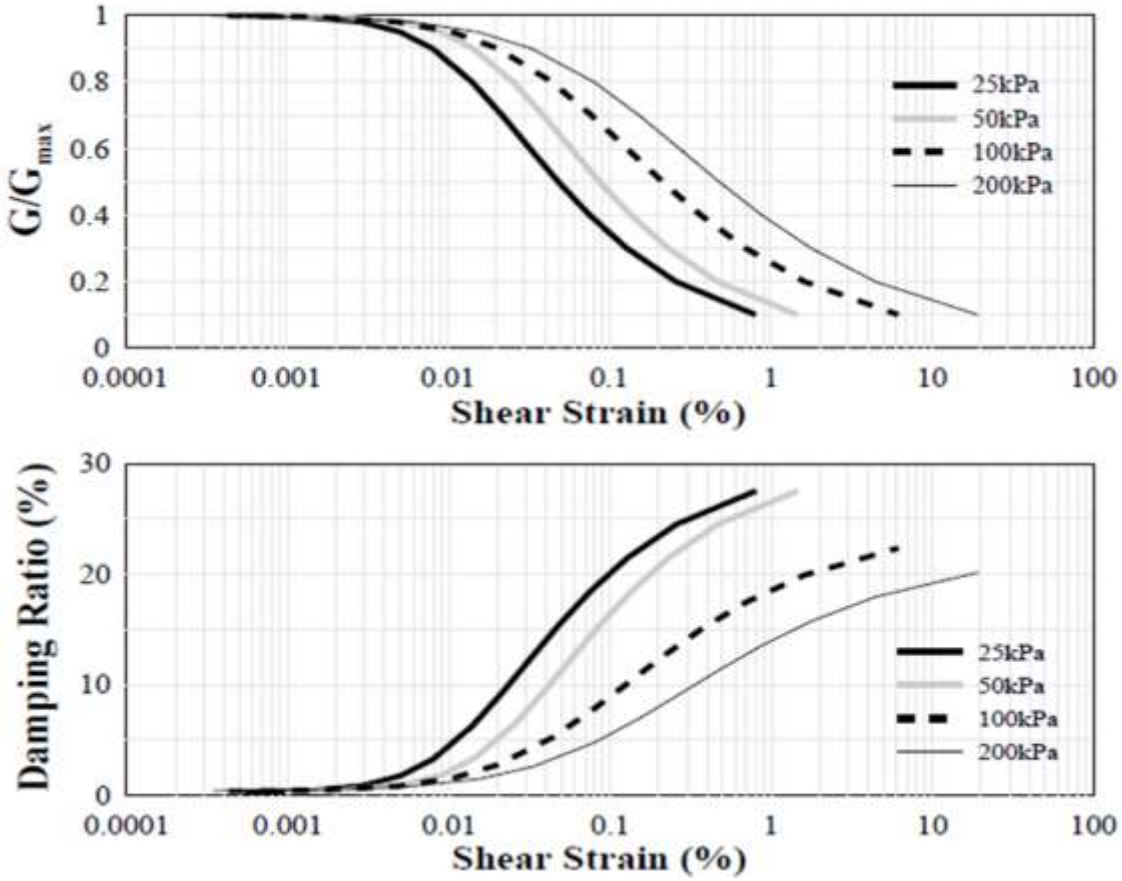

Figure 2.5 Degradation curves of shear modulus and damping ratio (Kim et al, 2013)

2.5 Mathematical Models for Large Strains: Non Linear Models

The linear behavior of the soil is only valid for very small level of strain. Therefore, the deformations induced by a seismic motion in the soil can easily reach the limit of its linear elastic domain. Consequently, it is very important to develop methods for taking into account the non-linearity of the soil in the problem of the dynamic soil-structure interaction, especially for moderate to strong motions able to induce damage on the superstructure. With the aim of making a simplified dynamic soil-structure interaction analysis, instead of a complete costly numerical modelling which includes the soil and the superstructure, it is possible to model the soil by springs which have equivalent characteristics (Winkler's springs approach). Thus, in order to take into account the nonlinear behavior of the soil, the use of springs with bilinear elastoplastic behavior is investigated. For each simplified model,

two sets of springs are used: one for vertical displacements and the other for the horizontal one.

2.6 The difference between linear and nonlinear soil Modeling

The first techniques used for dynamic soil analysis were linear and equivalent-linear methods. They utilized equivalent dynamic stiffness and hysteretic damping ratio as soil parameters. Development of computational means promoted the use of powerful numerical techniques for dynamic soil analysis, such as a step by step integration or true nonlinear methods. These methods involve tangent dynamic stiffness rather than the equivalent (secant) value. The tangent stiffness dependency on the shear strain amplitude, γ, can, in principle, be obtained from the experimental equivalent (secant) stiffness strain relationship (Gandomzadeh, 2011).

Site response analysis methods with nonlinear responses can be divided into the equivalent linear and nonlinear approaches. The first approach, the equivalent linear approach, approximates the nonlinear cyclic responses of soil samples. The effective shear strain is iteratively computed by updating the shear modulus and damping, after which the site response is simply estimated in the frequency domain. Given that the appropriate selection of the equivalent soil stiffness and damping for soil layers only represents a particular state in the stress-strain space and not the entire stress-strain evolution, this method fails to predict large plastic deformations of soil columns over the entire duration of a seismic event, and its use is strictly limited to relatively small shear strains or small nonlinearities (Hartzell, S. et al, 2004), (Hashash, Y.M.A.; Park,D., 2002)

The second approach, in which the soil dynamic characteristics are captured through a nonlinear hysteretic constitutive relationship, can represent the strain-dependent shear modulus and damping ratio. The simplest constitutive relationship uses a model relating the shear stress to the shear strain, whereby the backbone curve is expressed by a hyperbolic function. Several functions with empirical fitting parameters have been proposed to describe the strain-dependent response defined by the backbone curve, (Darendeli, 2001). More sophisticated models for cyclic loading use more fitting parameters so as to precisely

reproduce closed hysteresis loops that are influenced by basic soil parameters (plasticity, void ratio, confinement stress) and the imposed shear strain amplitude (Chong, Song-Hun, 2017).While those models are capable of expressing the nonlinear hysteretic response or degree of strain-dependence during steady-state cyclic loading, their input parameters lack both a physical basis and robustness, and the use of such models is quite limited to certain soils.

In large strain range (Figure 2.6a) significant changes occur in the soil microstructure (grain rearrangement) inducing irrecoverable shear and volumetric strains.

These changes induce settlements in dry or unsaturated soils and pore pressure build up in saturated impervious soils. Pore pressures may rise to a condition where the effective stresses become equal to zero and, consequently, the soil shear resistance drops to a very small value; this phenomenon is known as liquefaction. Even if liquefaction is not reached, the pore pressure increase induces a drop in the soil stiffness These two factors, shear stiffness degradation and loss of shear strength, make saturated soils subjected to strains larger than highly nonlinear. This behavior, with irrecoverable strains, can only be described with nonlinear models.

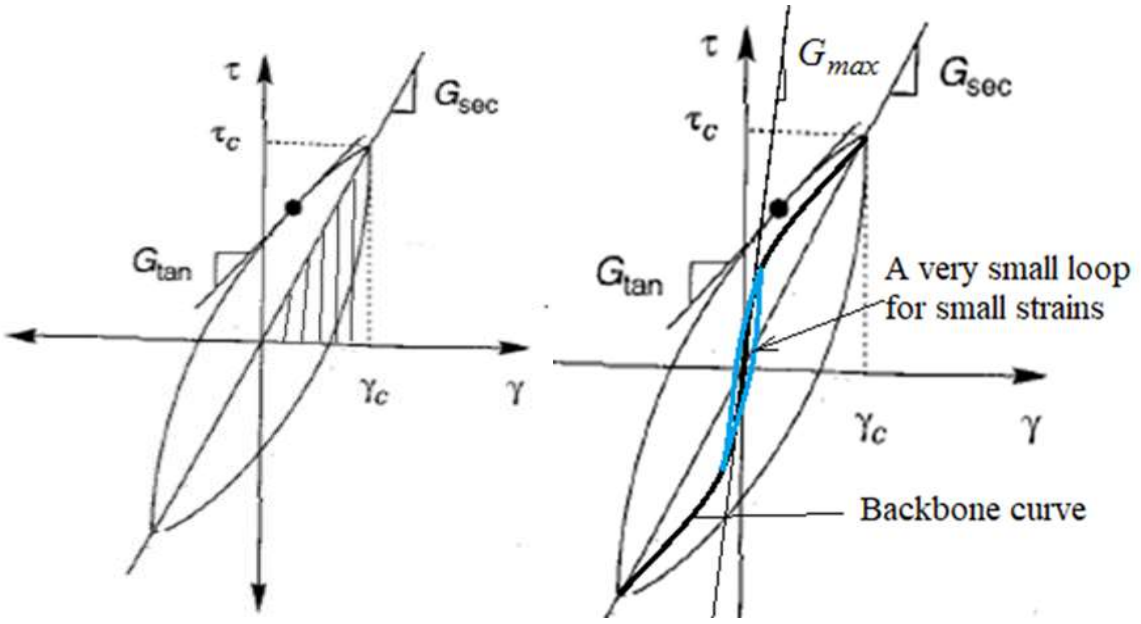

(a) (b)

Figure 2.6 Comparisons between small strain (b) and large strain (a) Response of the soil

2.6 Characteristics of Fully Nonlinear (Large strain) Modeling

It is widely recognized that nonlinear time-history analysis constitutes the most accurate way for simulating response of structures subjected to strong levels of seismic excitation. This analytical method is based on sound underlying principles and features the capability of reproducing the intrinsic inelastic dynamic behaviour of structures.

The following characteristics of the fully nonlinear method are helpful in nonlinear dynamic loading than either of the equivalent linear or linear method of analysis (Itasca, 2012)

1. The method follows any prescribed nonlinear constitutive relation. If a hysteretic type model is used, and no extra damping is specified, then the damping and tangent modulus are appropriate to the level of excitation at each point in time and space, since these parameters are embodied in the constitutive model.
2. Using a nonlinear material law, interference and mixing of different frequency components occur naturally.
3. Irreversible displacements and other permanent changes are modeled automatically.
4. A proper plasticity formulation is used in all the built-in models, whereby plastic strain increments are related to stresses.
5. The effects of using different constitutive models may be studied easily.
6. Both shear and compressional waves are propagated together in a single simulation, and the material responds to the combined effect of both components. For strong motion, the coupling effect can be very important. For example, normal stress may be reduced dynamically, thus causing the shearing strength to be reduced, in a frictional material.

2.7 Dynamic response of vertically loaded nonlinear pile

The deformations induced by a seismic motion in the soil can reach the limit of its linear elastic behavior and thus it is necessary to take into account its nonlinear behavior in the dynamic soil-structure interaction problem (DSSI). Consequently, it is very important to develop methods considering the non-linearity of the soil in the DSSI, especially for moderate to strong motions, able to induce damage on the superstructure (Ali

Gandomzadeh et al, 2008). In general, under earthquake loading, the soil reaches the limit of its elastic behavior before the structural elements. Thus, an earthquake analysis approach assuming nonlinear structural behavior under fixed base condition or with linear soil-structure interaction (SSI) hypothesis is not consistent.

In practice, there are several approaches to estimate the effect of the nonlinear soil behavior on the seismic response of structures. Usually, 2D finite element computations assuming plane-strain condition for the soil can be carried out in order to assess the role of the non-linear soil behavior on the superstructure response.

The major full-scale field testing carried out on piles embedded in clay and sandy clay sites by (Adimoolam et al, 2013) and clearly demonstrate that the performance of existing linear and nonlinear models are highly dependent on in-situ soil nonlinearity and dynamic loading characteristics. Hence, conducting in-situ full-scale dynamic tests on piles in order to have a better understanding of nonlinear response of piles should accurately assess the dynamic characteristics of soil-pile system.

When a harmonic load of amplitude, Q, is applied at the pile head, the slippageness of the soil increases the maximum pile-head displacement and changes the phase shift (Mohammad M . Ahmedin and Mahdi Ehsan, 2008).This is so by assuming that the nonlinearity of the response is due to the interaction between the pile and the soil medium. When severe nonlinearity develops in end bearing piles, the real part of the stiffness is reduced to the stiffness of a pile shaft alone and the imaginary part increases very little with frequency. When severe nonlinearity develops in floating piles, the real part of the stiffness is drastically reduced to a very small number and the imaginary part increases with frequency even faster than it does under elastic conditions (Mohammad M . Ahmedin and Mahdi Ehsan, 2008).

Evaluation of the behavior of PSS for lateral dynamic loading of nonlinear response was investigated by (Adimoolam et al, 2013)using the major full-scale field testing and they tried to validate the results of the field test using numerical methods (ABQUS) and they conclude that the simulated response matches fairly well with the measured response at low to moderate force levels, the simulated response at higher force level is 30% more than that measured in the field.

Many sophisticated linear and nonlinear models were proposed to study the lateral response of piles under dynamic loads (Adimoolam et al, 2013), (Rini Kusumawardani et al, 2015) and linear vertical models were proposed (Fekadu, 2010). And concluded that the deformation of the pile increased with the frequency of vibration and when it reaches at a particular frequency remains constant and further increment of frequency leads to a decrement of the corresponding deformation. But they have a short coming of modeling numerically the soil pile system in nonlinear model for vertical loading.

In this research, therefore, is intended to come up with the behavior of pile loaded vertically in nonlinear stage of loading condition by varying the frequency of loading with a particular dynamic load.

2.8 Soil Pile Interaction

During seismic loading the soil undergoes deformations which are imposed to the foundation; the question naturally arises of knowing if the motion in the vicinity of the structure is altered by the presence of the structure and how the structure response is modified by the compliance of the supporting soil. This interaction between the structure and the soil is named soil-structure interaction (SSI). The dynamic loads applied to the foundation arise from the inertia forces developed in the superstructure and from the soil deformations, caused by the passage of seismic waves, imposed on the foundations. These two phenomena are referred in the technical literature as inertial and kinematic loading. The relative importance of each factor depends on the foundation characteristics and nature of the incoming wave field.

3 METHODOLOGY

3.1 General

In linear elasticity problems, the stiffness matrix is constant which brings linear element equations. But Soil in nature is a nonlinear material. Therefore, If the soil is nonlinear elastic/ or elasto plastic, the equivalent constitutive matrix is no longer constant, hence varies with stress and/or strain. It is, therefore, changes during a finite element/ Finite difference analysis. Consequently, a solution strategy is required which can account for this changing material behavior. This strategy is a key component of nonlinear finite element/ Finite difference analysis, as it can strongly influence the accuracy of the results and the computer resource required to obtain them. Thus the problem can be solved by applying all the loads in a single calculation step. (Mohammad M . Ahmedin and Mahdi Ehsan, 2008).

3.2 Soil-pile system Modeling

In this section, the 3D mesh, boundary conditions and properties of soil and that of pile was discussed. Of which the soil properties are the same as (Kim et al, 2013). the pile which is embedded at the center of the soil block was inserted with **sel** command of the computing tool called FLAC ^{3D}.

3.2.1 Finite Difference Model

The modeling of geomechanics problems involves media which, at the scale of the analysis, are better represented as unbounded. Deep underground excavations are normally assumed to be surrounded by an infinite medium, while surface and near-surface structures are assumed to lie on a half-space (dams for example). Numerical methods relying on the discretization of a finite region of space requires appropriate conditions to be enforced at the artificial numerical boundaries. In static analyses, fixed or elastic boundaries can be realistically placed at some distance from the region of interest. In dynamic problems, however, such boundary conditions cause the reflection of outward propagating waves back into the model and do not allow the necessary energy radiation (Itasca, 2012). The use of a larger model can minimize the problem, since material damping will absorb most of the energy in the waves reflected from distant boundaries (Itasca, 2012). To overcome on such

problems, accordingly, rather than adding quite boundary a very large three-dimensional geometric model was used to represent the soil-pile system. Soil and pile were modeled using eight-node block elements. The size of the block was taken as 20m x 20m x 20m and of which on the half depth of the block, 10m, and structural pile was inserted having the length of 10m.

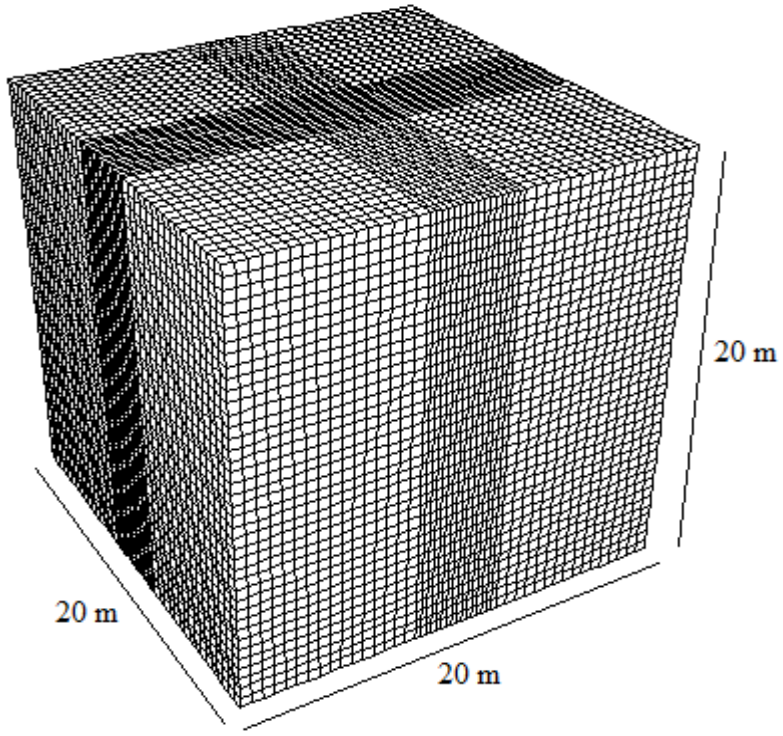

Figure 3.1 Three dimensional model of geometry of soil block.

3.2.2 Soil Elements

Brick zone elements were used in this study, a brick of size 20m x 20m x 20m were used and eight nodded brick sizes were generated depending on the mesh size decided. Brick element mesh shape has the lowest absolute error and tetrahedral has the highest (Itasca, 2012) that is why brick element was preferred. FLAC^{3D} uses a mixed discretization technique to overcome overlay stiff elements and give elements more volumetric flexibility without introducing unconstrained degrees-of-freedom. In mixed discretization, a zone is made of an assembly of two overlapping groups of tetrahedrons, as illustrated in Figure 3.2.

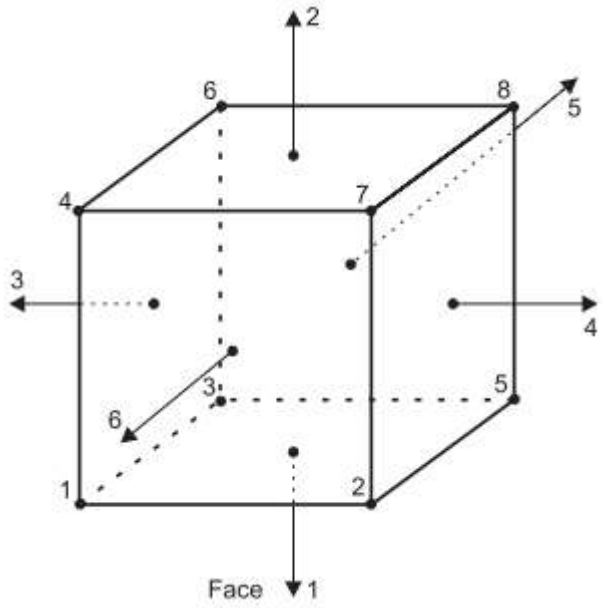

Figure 3.2 Brick element zones with 5 tetrahedral, (Itasca, 2012)

Table 3.1 Summery of soil properties after experimental test (Kim et al, 2013)

Unit weight (kN/m^3)	Cohesion (kN/m2)	Internal Friction Angle(°)	Poisons Ratio	Shear wave velocity (m/s)
15.21	0	43	0.25	189

The soil parameters used, however, are not linear as the nonlinear response of soil for dynamic loading was targeted and hence the modulus reduction function is required. Such reduction functions with respect to Shear modulus and damping coefficient are given in table 3.2.

3.2.3 Maximum shear modulus

The maximum shear modulus of the materials were calculated based on a model that gives the maximum shear modulus as a function of the confining pressure and the maximum value of the acceleration history, which is a function of relative densities if different materials are used for a particular model. For a single material, however, a single maximum shear

modulus is going to be taken with the corresponding confining pressure. In this research, therefore, it was intended to take a particular maximum shear modulus with the confining pressure with which the laboratory results of the soil incorporates in the model was made. The maximum shear modulus of 37.36 mPa was taken. This maximum dynamic shear modulus of the soil was investigated in such way that its value was varied with in depth and it became constant after some depth, 37.36 mPa, (Kim et al, 2013) and hence this value was taken for modeling of this task because the properties of the top soil layers greatly governs degree of nonlinearity and the dynamic lateral stiffness of the soil-pile system (Boominathan A. and Ayothiraman R., 2006). Hence this value of maximum dynamic shear modulus value was interpreted to appropriate values modulus of elasticity and bulk elastic modulus provided that the modulus of elasticity is in between the range of dense sand soil .the corresponding elastic properties were determined using equation 3.1 and 3.2 bellow and then coded in FLAC^{3D} .

$$G = \frac{E}{2(1+v)} \qquad 3.1$$

$$K = \frac{E}{3(1-2v)} \qquad 3.2$$

Where

G is the shear modulus

K is the bulk modulus

E is the young's modulus (modulus of elasticity) and

V is the poisons ratio

$$G = \frac{E}{2(1+0.25)} \Rightarrow 2.5G = E$$

$$2.5 * 37.36 = E \quad \Rightarrow E = 93.4\ MPa$$

The bulk modulus of the soil is then,

$$K = \frac{93.4\ MPa}{3(1 - 2 * 0.25)} = \ \ 62.267\ MPa$$

3.2.4 Strain Dependency of Dynamic Shear modulus

The damping shear modulus of the analysis while encoding in FLAC^{3D} should be in appropriate relation with in the cyclic shear strain. The locus of points corresponding to the tips of hysteresis loops of various cyclic strain amplitudes is called a backbone (or skeleton) curve. Characterization of the stiffness of an element of soil requires consideration of both G_{max} and the way the modulus ratio G/G_{max} varies with cyclic strain amplitude and other parameters. The variation of the modulus ratio with cyclic shear strain is described by a modulus reduction curve. The nonlinear stress-strain behavior of soils can be represented more accurately by cyclic nonlinear models that follow the actual stress-strain path during cyclic loading. Such models are able to represent the shear strength of the soil, and with an appropriate pore pressure generation model, changes in effective stress during undrained cyclic loading. A variety of cyclic nonlinear models have been developed; all are characterized by 1) a backbone curve and 2) a series of rules that govern unloading-reloading behavior, stiffness degradation, and other effects. Alternatively, backbone curves can be constructed from modulus reduction curves and vice versa. (Darendeli, 2001)

The backbone curve can be expressed in a variety of ways, either in terms of a mathematical function or in terms of discrete stress-strain coordinates for purposes of soil applications, several simple mathematical functions have been proposed. These include the bilinear, the multilinear, the hyperbolic, the Ramberg-Osgood and logarithmic formulations. Hyperbolic function was one of the earliest proposition presented by (Hardin and Drench, 1985) believed that the two-constant hyperbolic form of the stress-strain that they presented is such that the ultimate shear strength of the soil is contained within the general formulation and appears in the mathematical limit of the stress as the strain becomes excessive. According to Hardin and Drench, the original hyperbolic function of backbone curve is represented by an equation (Itasca, 2012),

$$F_{bb}(\gamma) = \frac{G_0\gamma}{1 + \left(\frac{G_0}{\tau_{max}}\right)|\gamma|} \qquad 3.3$$

Which concludes the shear modulus reduction curve produces equation 3.4 bellow,

$$G(\gamma) = \frac{G_0}{1 + \left|\frac{\gamma}{\gamma_{ref}}\right|} \qquad 3.4$$

Where γ_{ref} is equal toτ_{max}/G_0.

Some models, however, require numerous parameters that are difficult to determine accurately in practice. Furthermore, they tend to be quite sensitive to the chosen values of the material parameters (Ronaldo I. Borja, 2000). The latter point is crucial since even the simplest form of non-linear material characterization, the degradation of shear moduli with shear strain, can be difficult to establish accurately in practice unless one performs very careful laboratory experiments. Considering that there is a large variation in the amount of site-specific information available for estimating ground motion at a site, it is important to start with a simple enough non-linear soil model such as the one indicated in this paper.

Table 3.2 Summery of test results of soil used for modeling (Kim et al, 2013)

Cyclic Shear Strain (%)	0.001	0.01	0.03	0.1	0.3	1	3	6
Shear Reduction Function (G/G_{max})	1	0.96	0.86	0.65	0.45	0.26	0.15	0.1
Damping Ratio (%)	0.05	2	4	8.5	14	18.6	20.5	22.5

3.2.5 Model Setup and material encoding for dynamic load analysis

Here to set up the modeling of the pile in to FLAC^{3D}, it was found to be necessary to determine the appropriate size of meshing as it depends on the wave length and shear wave velocity of vibration. The length of the elements should not exceed the wave length of the wave to be applied at the peak of the pile. It is recommended that the size of the elements must be inside the range $\left(\frac{1}{10} - \frac{1}{8}\right)\lambda$ where λ is the wave length of the vibration. In this research, however, the reverse of what is known in earth quake vibration was executed

which happens at a particular frequency. Therefore, it is found that the maximum wave length in which energy dissipates has to be found Using equation 2.7, 2.8 and 2.9

$$\frac{L}{R} = \frac{10}{0.3} = 33.33 \; and \;\; \frac{E_p}{G} = \frac{30 * 10^9}{37.36 * 10^6} = 800$$

Results $f_{z1} = 0.035$ and $f_{z2} = 0.078$ from figure 2.3 and 2.4 respectively.

$$k_z = \left(\frac{30 * 10^9 * 0.2826}{0.3}\right) 0.035 = 989.1 * 10^6$$

And

$$C_Z = \left(\frac{E_P A}{v}\right) f_{z2} = \left(\frac{30 * 10^9 * 0.2826}{189}\right) 0.078 = 349.744 * 10^4$$

$$f_n = \left(\frac{1}{2\pi}\right)\sqrt{\frac{k_z}{m}} = \left(\frac{1}{2\pi}\right)\sqrt{\frac{989.1 * 10^6}{7200}} = 59.86 \approx 60Hz$$

The above values bring that the natural frequency is near to $60Hz$ and hence, one can be quite sure that beyond this frequency of vibration the dynamic response of the pile starts to decrease (A BOOMINATHAN And T LAKSHMI, 2000). In this particular work, therefore, it was intended to extend and tried to capture what will be happened until the frequency of vibration is 90 Hz. And hence using this much frequency of vibration it was very essential to check that weather the discretization size of the model captures it. The wave length was calculated as shear wave velocity divided by frequency that gives the maximum energy of shaking. Therefore, the corresponding wave length was calculated using the formula of: (Braja M. Das, G.V. Ramana, 2011)

$$\lambda = \frac{Vs}{f} \qquad 3.5$$

Where $V_{s.}$ is shear wave velocity in m/s and f is the frequency in Hertz and hence, using equation 3.3 above, it is possible to determine the wave length once the density and shear

wave velocity of the soil was tested and tabulated as in table 3.3 by varying the frequency of loading.

Table 3.3 Appropriate meshing size of the model

Material Description	Shear velocity(Vs.)(m/s)	Frequency (Hertz)	Wave length (λ)	Size(m) $\lambda/10$	Size(m) $\lambda/8$
		1	189	18.9	23.625
		10	18.9	1.89	2.363
		20	9.45	0.945	1.18
		30	6.3	0.63	0.788
		40	4.725	0.473	0.591
		50	3.78	0.378	1.51
Uniform Sand	189	60	3.15	0.315	0.394
		70	2.7	0.27	0.338
		80	2.363	0.236	0.295
		90	2.1	0.21	0.265

So it was recommended to use the mesh size in between 0.21 m and 0.265 m and hence 0.25m mesh size was used near to the pile and increased twice as away from the center for simplicity of calculation. The subdivisions of the discretization were kept fine near to the center of the block, 0.25m size of discretization, to allow for an even distribution of vertically and horizontally propagation SH waves and as the block of the soil is far away from the area where the vertical dynamic load is induced, the speed of propagation of wave is decreased and hence the discretization size has been increased to 0.5 m, as shown in figure 3.2 bellow.

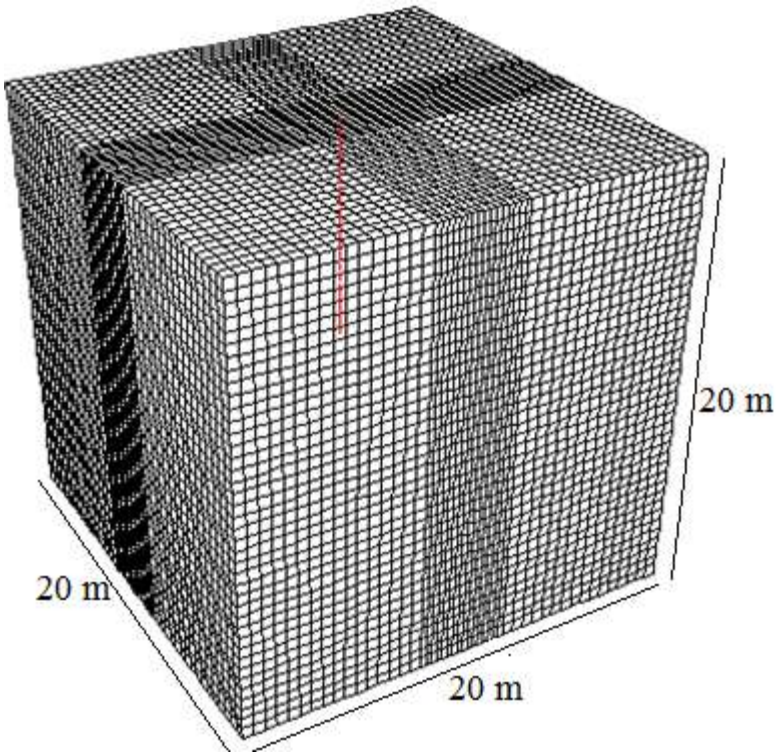

Figure 3.3 Soil block of the model with appropriate meshing size having a pile at the center of the block

3.2.6 Pile Element

3.2.6.1 Mechanical Behavior of pile structural element in FLAC ^{3D}

Pile structural element is defined by its geometric, material and coupling-spring properties. A Pile structural element is assumed to be a straight segment of uniform bisymmetrical cross-sectional properties lying between two nodal points. An arbitrarily curved structural pile can be modeled as a curvilinear structure comprised of a collection of pile structural elements. The stiffness matrix of a pile structural element is identical to that of a beam, however, in addition to providing the structural behavior of a beam (including the ability to specify a limiting plastic moment), both a normal-directed (perpendicular to the pile axis) and a shear-directed (parallel with the pile axis) frictional interaction occurs between the pile and the grid. In this sense, piles offer the combined features of beams and cables (Itasca, 2012). In addition to skin-friction effects, end-bearing effects were also be modeled. Pile structural elements are suitable for modeling structural-support members, such as foundation piles, for which both normal and shear-directed frictional interaction with the

soil mass occurs. Each Pile structural element has its own local coordinate system, shown in Figure 3.3. The Pile structural element coordinate system was defined by the locations of its two nodal points, labeled 1 and 2 in Figure 3.3. Piles interact with the grid via shear and normal coupling springs. The coupling springs are nonlinear, spring-slider connectors that transfer forces and motion between the pile and the grid at the pile nodes (by way of the link emanating from each pile node). The behavior of the normal coupling springs includes the ability to model load reversal and the formation of a gap between the pile and the grid. The normal coupling springs can simulate the effect of the host medium squeezing around the pile.

3.2.6.2 Properties of the pile used for modeling

Unlike soil elements, elastic concrete material was used to simulate the pile material. Table 3-4 shows material properties of the pile used in this model and the pile system, unlike soil block, can be generated using structural element (SEL command, see the command attached in the appendix) in FLAC ^{3D} finite difference software.

Table 3.4 Pile material properties after (Mamo, 2016.)

Parameters	Value(s)	Unit
Material Model	Linear Elastic	-
Unite weight(C-30 Concrete)	25	kN/m^3
Modulus of Elasticity(E)	30	GPa
Poisson's ratio(v)	0.20	-

A pile of twenty nodes having the properties of table 3.4 was then generated at the center of the block as shown in the figure 3.3 bellow

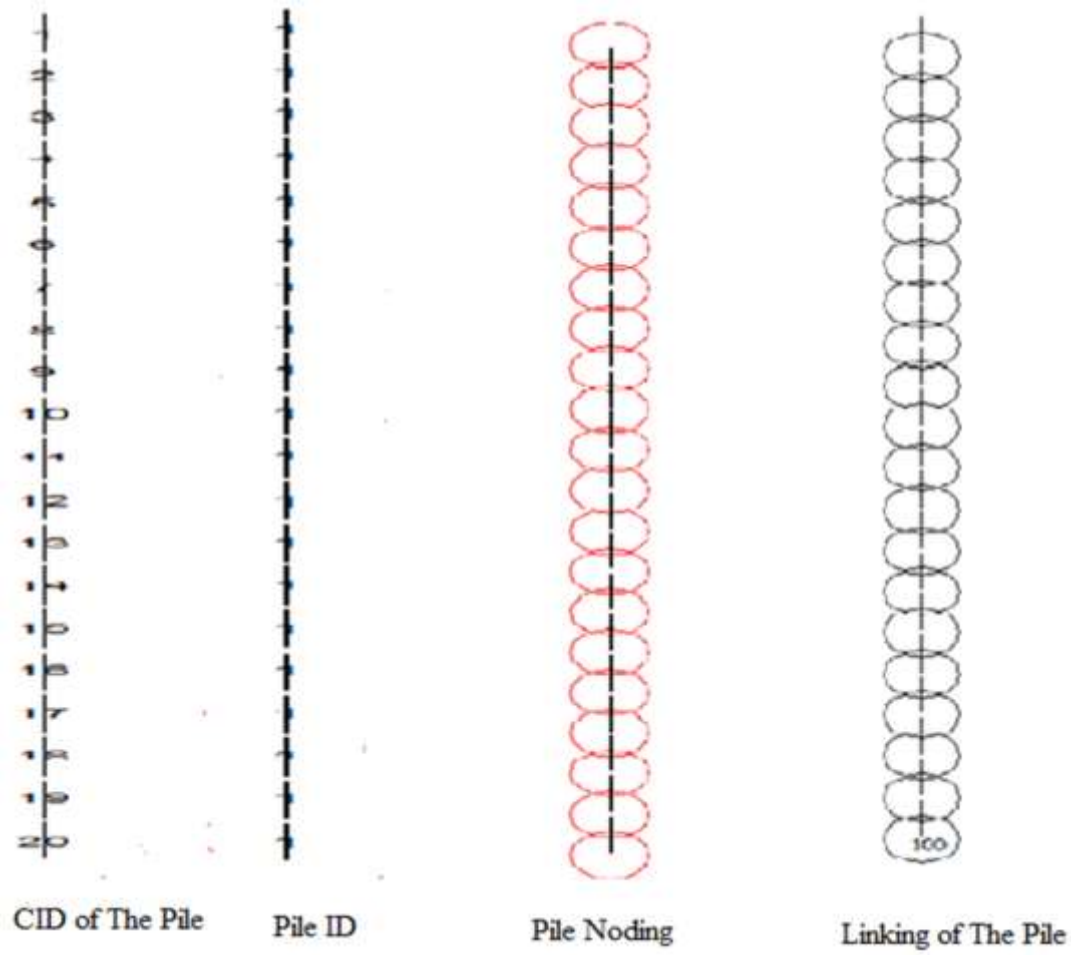

Figure 3.4 Structural element of pile having different properties

3.2.7 Boundary conditions

Boundary conditions are applied to those regions of the model where the displacements and/or rotations are known. Such regions may be constrained to remain fixed (have zero displacement and/or rotation) during the simulation or may have specified, nonzero displacements and/or rotations when expected to subjected with already known corresponding parameters. Thus, in this particular work, a fixed boundary is set at the bottom and at the sides of the soil region of the model. The pile, however, was completely embedded in the soil region and it was assumed to be bearing on the similar soils of which it has embedded in. Therefore all the bearing nodes were replaced with springs of having an equivalent sub grade reaction of the soil on which the pile is embedded as shown in figure 3.6 bellow. It was assumed that the soil and pile are perfectly bonded. The side boundaries

of the block soil in which pile is intended to install are constrained against horizontal direction and the bottom boundaries are constrained against both Horizontal and vertical directions. Also, quiet boundaries are used for wave propagation and to eliminate "box effects'' (i.e. the reflection of waves back into the model at the boundaries). In this research, however, since the model is very large there will no probability of the reflection of wave and hence in such case it is not necessary to use quite boundaries. To apply the quiet boundaries to the model, infinite elements are used at the boundaries.

3.2.8 Interfaces

FLAC^{3D} provides interfaces that are characterized by Coulomb sliding and/or tensile and shear bonding. Interfaces have the properties of friction, cohesion, dilation, normal and shear stiffness's, tensile and shear bond strength. *FLAC*^{3D} represents interfaces as collections of triangular elements (interface elements), each of which is defined by three nodes (interface nodes). Interface elements can be created at any location in space. Generally, interface elements are attached to a zone surface face; two triangular interface elements are defined for every quadrilateral zone face. Interface nodes are then created automatically at every interface element vertex. When another grid surface comes into contact with an interface element, the contact is detected at the interface node, and is characterized by normal and shear stiffness's, and sliding properties. Each interface element distributes its area to its nodes in a weighted fashion. Each interface node has an associated representative area. The entire interface is thus divided into active interface nodes representing the total area of the interface which can be shown as in figure 3.5 bellow

Here in this particular work, Interface was created with the **INTERFACE** command in FLAC^{3D} between pile and pile cap while the validation model was developed such that the normal and shear spring constants were taken as the stiffest material. This was so to attach an interface to one of the grid surfaces. This command generates interface elements for interface along all surface zone faces with a center point that fall within a specified range. Any surfaces on which an interface is to be created must be generated initially.

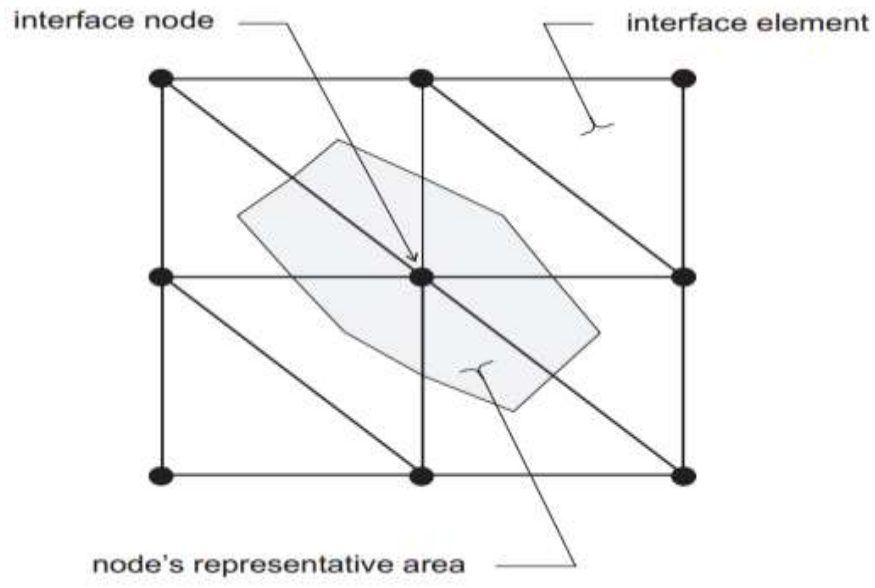

Figure 3.5 Distribution of representative areas to interface nodes (Itasca, 2012)

3.2.8.1 Assigning interaction (SPI) Properties

The pile was simulated by the pile element in the FLAC^{3D} and set at the center of the model. During the interaction of pile and soil, the pile bears the axial pressure, axial friction force, and transverse shear. The pile was divided into micro segments of equal length, 0.5m, which were used in the elastic plastic analysis. Finally, the stress-strain response of the whole pile was obtained by the integral accumulation effect. Piles interact with the soil via shear and normal coupling springs. The coupling springs are nonlinear, spring-slider connectors that transfer forces and motion between the pile and the grid at the pile nodes (by way of the link emanating from each pile node). The normal and shear behavior of the pile-grid interface is cohesive and frictional in nature. The behavior of the normal coupling springs includes the ability to model load reversal and the formation of a gap between the pile and the grid. The normal coupling springs can simulate the effect of the host medium squeezing around the pile (Itasca, 2012). The shear behavior of the grout annulus, during relative shear displacement between the pile/grout interface and the grout/soil interface, is described numerically by stiffness, cohesive strength, friction angle, and exposed perimeter. The equivalent linear dynamic behavior of SPI during earthquake has been used,

The interaction between contacting surfaces of pile and soil consists of two components: one normal to the surfaces and the other tangential to the surfaces. The tangential component consists of the relative motion (sliding) of the surfaces and, possibly, frictional shear stresses. The contact constraint has been applied in FLAC ^{3D} using the slide command (See the command attached in the Appendix A). For normal interaction, on the other hand, the equivalent spring having a subgrade reaction modulus is assigned after the link of the pile node at where the pile have end bearing node is deleted (also see the command attached in the appendix A). The equivalent subgrade reaction modulus of the pile after installed with the spring used for this particular modeling was calculated in equation 3.8 bellow.

The interface between the pile and the soil was characterized by Columb sliding as stated in the previous section. For this, K_n and K_s values were computed by the approach indicated in the manual of FLAC^{3D}. The bulk and shear modulus of the stiffest neighboring zone was computed using equations 3.1 and 3.2

The young's modulus of the stiffest neighboring zone for the interface was 30 GPA (the stiffest of the soil and concrete pile). The Poisson's ratio of this material was considered as 0.2. Inserting these two values in to equations 3.6 and 3.7, the values of G and K were computed as

$$G = \frac{30 * 10^9 Pa}{2(1 + 0.2)} = 12.5 * 10^9 Pa$$

$$K = \frac{30 * 10^9 Pa}{3(1 - 2 * 0.2)} = 16.67 * 10^9 Pa$$

A good rule-of-thumb is that k_n and k_s be set to ten times the equivalent stiffness of the stiffest neighboring zone. The apparent stiffness (expressed in stress per-distance units) of a zone in the normal direction is (Itasca, 2012),

$$k_n = k_s = 10 \max\left(\frac{k + {}^4/_3\, G}{\Delta z_{min}}\right) \qquad 3.6$$

Hence $\Delta z_{min} = 0.5$m.

Substituting now the value of K and G in equation 3.6

$$k_n = k_s = 10 \max\left(\frac{16.67 * 10^9 Pa + {}^4/_3\,(12.5 * 10^9 Pa)}{0.5m}\right) = 6.67 * 10^{11} N/m$$

The exposed perimeter of a pile element and the properties of the coupling springs were chosen to represent the behavior of the pile/medium interface commensurate with the problem being analyzed. For piles in soil, the PSI can be expressed in terms of a shear response along the length of the pile shaft as a result of axial loading (e.g., a friction pile), or in terms of a normal response when the direction of loading is perpendicular to the pile axis (e.g., piles used to stabilize a slope). PSI will depend on whether the pile was driven or cast-in-place. The interaction is expressed in terms of the shear resistance that can develop along the length of the pile. For example, driven friction piles receive most of their support by friction or adhesion from the soil along the pile shaft. A cast-in-place end-bearing pile, on the other hand, receives the majority of its support from soil near the tip of the pile. In many cases, properties needed to describe the site-specific response of the PSI will not be available. However, a reasonable understanding of the soil properties at the site is usually provided from standard in situ and laboratory tests. In such cases, the pile/soil shear response can be estimated from the soil properties (Itasca, 2012). If the failure associated with the pile/soil response is assumed to occur in the soil, then the lower limits for cs sfric and cs scoh can be related to the angle of internal friction of the soil (for cs sfric in appendix A) and the soil cohesion times the perimeter of the pile (for cs scoh in appendix A). If failure is assumed to occur at the pile/soil interface, the values for cs sfric and cs scoh may be reduced to reflect the smoothness of the pile surface.in this research, however, since the soil where the pile was embedded in is sandy soil, it is pure of any doubt as the above value cs scoh of zero and in the case of cs sfric was assigned and hence are encoded in the FLAC^{3D} (See the command attached in the appendix A)

3.2.8.2 End Bearing

The ultimate bearing capacity due to end-bearing resistance of a single pile is typically calculated based on the principles of bearing capacity for shallow foundations. For a single pile in a chohesionless soil, the end-bearing capacity,Q_p, is given by (Cernica, 1995)

$$Q_p = A_p \gamma L N_q \qquad 3.7$$

Where A_p = area of pile tip

$$N_q = \left(\frac{1 + sin\phi}{1 - sin\phi}\right)^2, \qquad where\ \varphi\ is\ the\ friction\ angle\ of\ the\ soil$$

Produces $Q_p = 359.07$ kN which is end bearing of the soil at the end of the pile, coded in the FLAC ^{3D} (see the command attached at the appendix A)

3.2.8.3 Wave Transmission

Numerical distortion of the propagating wave can occur in a dynamic analysis as a function of the modeling conditions. Both the frequency content of the input wave and the wave speed characteristics of the system will affect the numerical accuracy of wave transmission. (Itasca, 2012) Show that, for accurate representation of wave transmission through a model, the spatial element size, Δl, must be smaller than approximately one-tenth to one-eighth of the wavelength associated with the highest frequency component of the input wave

$$\Delta l \leq \frac{\lambda}{10} \qquad 3.8$$

Where λ is the wavelength associated with the highest frequency component that contains appreciable energy. The frequency of vibration, therefore, is dependent on the Rayleigh damping and the natural mode of oscillation of the system. The fundamental frequency, *f*, associated with the natural mode of oscillation of a system is

$$f = \frac{Cs}{\lambda} \qquad 3.9$$

Where C_s = speed of propagation associated with the mode of oscillation; and λ = longest wavelength associated with the mode of oscillation. The size of discretization element, therefor was don accordingly as discussed in section 3.3

3.2.8.4 Checking Wave Transmission

The dynamic loading for this problem was a sinusoidal load applied at the top of the model in the down ward vertical direction. The wave had a maximum frequency of 90 Hz. The largest zone dimension for this model in the vertical direction was 0.5 m. based on Eqs. (3.7) and (3.8), Therefore, the frequency of vibration of the impute dynamic load should less than this frequency in such a way that the propagation of this wave was addressed appropriately with in a maximum vertical discretization size of 0.5 m and the maximum horizontal and transverse direction discretization of 0.25m. Hence, the corresponding wave lengths and size of the element is given in table 3.3 above.

3.2.8.5 Application of Dynamic Input

FLAC^{3D} models a region of material subjected to external and/or internal dynamic loading by applying a dynamic input boundary condition at either the model boundary or at internal grid points. Wave reflections at model boundaries may be reduced by specifying quiet (viscous) or free-field boundary conditions. In FLAC^{3D}, the dynamic input can be applied in one of the following ways:

(a) an acceleration history;

(b) a velocity history;

(c) a stress (or pressure) history; or

(d) a force history.

In this particular work, however, a vertical force history (Z-direction) just at the head of the pile was going to be applied and interested to observe the targeted out puts. a *FISH* function is used to provide the multiplier, the function must access dynamic time within the function, using the FLAC^{3D} scalar variable **dytime**, and compute a multiplier value that corresponds

to this time. In this research, therefor, a FISH function is intended to be used since the applied load is external and going to be applied at the head of the pile as discussed already.

3.2.8.6 Applying Vertical Dynamic (Excitation) Load

The loads are assumed to vary sinusoidally with time over 1-90 Hz of frequencies. Thus, the Mathematical equation of (Braja M. Das, G.V. Ramana, 2011)

$$\boldsymbol{Q} = Q[X\ sin(\omega t + \Phi o\ ) + iYcos\ (\omega t + \Phi 0\ )] \qquad 3.10$$

In which Q = Complex harmonic load Q = Input value of the load X, Y= Amplitude multipliers ω (Angular frequency) = 2ΠIf, with f = frequency in Hz, Φo = Initial phase angle in degrees in the sine function. In here, a dynamic load of 10 kN for a frequency range of 1-90 Hz is used provided that the dynamic vibrational load transferring mechanism depends on the type of pile in which the load is going to be applied.

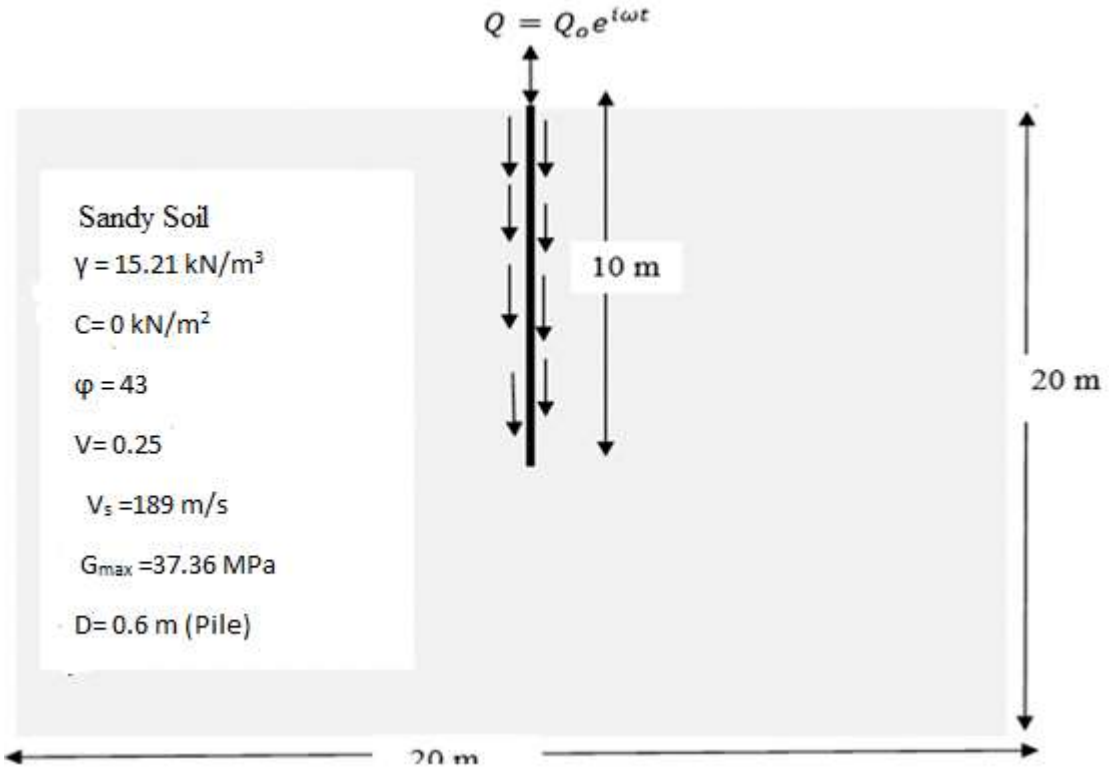

Figure 3.6 2D View of soil pile system

3.2.8.7 Dynamic time step

The calculation of critical time step is identical to that given

$$\Delta t_{crit} = \min\left\{\frac{V}{C_p A^f{}_{max}}\right\} \qquad 3.11$$

Where

$$C_p = \sqrt{\frac{k + \left(\frac{4G}{3}\right)}{\rho}} \qquad 3.12$$

V is the tetrahedral sub-zone volume, and $A^f{}_{max}$ is the maximum face area associated with the tetrahedral sub-zone. The min {} function is taken over all zones and includes contributions from the structural and interface modules.

3.2.8.8 Dynamic Multi-stepping

The maximum stable time step for dynamic analysis was determined by the largest material stiffness and smallest zone in the model (Eq. 3.10). Often, the stiffness and zone size can vary widely in a model.in this research, for example, the pile which is concrete and the soil block are interacted in which the variation of the stiffness is very large. In addition the size of discretized sub regions near to the center of the pile and away from are also varied with factor of two. A few zones, therefore, will then determine the critical time step for a dynamic analysis even though the major portion of the model can be run at a significantly larger time step. While such conditions are emanated, A procedure called dynamic multi-stepping is available in FLAC^{3D} to reduce the computation time required for a dynamic calculation. In this procedure, zones and grid points in a model are ordered into classes of similar maximum time steps. Each class is then run at its time step and information is transferred between zones at the appropriate time. Dynamic multi-stepping uses a local time step for each individual grid point and zone. At the start of an analysis, the grid is scanned and the local stable time step for each grid point,Δt_{gp}, is determined and stored. The value of Δt_{gp} depends on size, stiffness and mass of the neighboring sub-zones (as shown in Eq. 3.10), attached structural elements and interfaces. The global time step, Δt_G is determined as the

minimum of all Δt_{gp}, as in the standard formulation.so in order to get this time step of calculation, here under, invoking the command **SET dyn multi on** is essential and was done (see the command attached in the appendix A).

3.2.9 Mechanical Damping

Natural dynamic systems contain some degree of damping of the vibration energy within the system; otherwise, the system would oscillate indefinitely when subjected to driving forces. Damping is due, in part, to energy loss as a result of internal friction in the intact material and slippage along interfaces, if these are present. For a dynamic analysis, therefore, the damping in the numerical simulation should reproduce in magnitude and form the energy losses in the natural system when subjected to a dynamic loading. In soil and rock, natural damping is mainly hysteretic which is independent of frequency (Itasca, 2012)

3.2.9.1 Local damping

Local damping was originally designed as a means to equilibrate static simulations. However, it has some characteristics that make it attractive for dynamic simulations. It operates by adding or subtracting mass from a grid point or structural node at certain times during a cycle of oscillation; there is overall conservation of mass, because the amount added is equal to the amount subtracted. Mass is added when the velocity changes sign and subtracted when it passes a maximum or minimum point. Hence, increments of kinetic energy are removed twice per oscillation cycle (at the velocity extremes). So 5% damping was used, which is a typical value used for dynamic analyses and common for concrete structures.

3.2.10 Constitutive model

The nonlinear soil model, in the dynamic loading case can be modeled in either of the three case of Default model (the default FLAC^{3D}) modulus reduction function, Sig3 (sigmoidal model of having three parameters), sig4 (sigmoidal model of having four parameter), Hardin/Drnevich model, suggested by (Hardin and Drench, 1985)and etc. In this paper, however it is intended to model using the one with Sigmoidal (Sig4) was used.

3.2.10.1 Sigmoidal (Sig4) Model

Sigmoidal curves are monotonic within the defined range, and have the appropriate asymptotic behavior. Thus the functions are well-suited for the purpose of representing modulus degradation curves.so once the soil shear modulus reduction function with relation to cyclic shear strain is determined by whatever means, in this case laboratory tests, it is possible to represent it in the FLAC^{3D} using the four constants of the soil non linearity Characterstics. These four parameters are determined mathematically after regeresional is done having the secant modulus of corresponding cyclic shear strain is taken using the equation 3.14 given bellow. (Itasca, 2012)

$$M_s = y_0 + \frac{a}{1 + \exp\left(-\frac{L - x_0}{b}\right)} \qquad 3.13$$

Where M_s is secant modulus

The hysteresis model is developed by noting that the S-shaped curve of modulus versus logarithm of cyclic strain can be represented by a cubic equation, with zero slope at both low strain and high strain. Thus, the secant modulus, *Ms.*, is

$$M_s = s^2(3 - 2s) \qquad 3.14$$

Where

$$S = {(L_2 - L)}/{(L_2 - L_1)} \qquad 3.15$$

And L is the logarithmic strain, $L = log_{10}(\gamma)$ 3.16

The parameters L_1 and L_2 are the extreme values of logarithmic strain, the values at which the tangent slope becomes zero. Thus, giving $L_1 = -3$ and L_2 = 0.778 means that the S-shaped curve will extend from a lower cyclic strain of 0.001% (10^{-3}) to an upper cyclic strain of 6% (0.778). Since the slopes are zero at these limits, it is not meaningful to operate the damping model with strains outside the limits. Having these parameters right now, at least four equations are developed since four unknown parameters are there.

1. When $\gamma = 0.001$, using equation 3.12,

$$L = log_{10}(0.001) = -3$$

Then substituting the value in equation 3.16 above gives,

$$s = \frac{0.778 + 3}{0.778 + 3} = \frac{3.778}{3.778} = 1$$

The secant modulus is, then

$$M_s = 1^2(3 - 2) = 1$$

Substituting this value back to equation 3.15 gives,

$$1 = y_0 + \frac{a}{1 + \exp\left(\frac{4+x_0}{b}\right)} \qquad 3.17$$

2. When γ=0.01, Using similar procedure as above

$$s = \frac{0.778 + 3}{0.778 + 3} = 1$$

$$1.216 = y_0 + \frac{a}{1 + \exp\left(\frac{2+x_0}{b}\right)} \qquad 3.18$$

3. When γ=0.1, then

$$0.457 = y_0 + \frac{a}{1 + \exp\left(\frac{1+x_0}{b}\right)} \qquad 3.19$$

4. When γ=1, then

$$0.11 = y_0 + \frac{a}{1 + \exp\left(\frac{x_0}{b}\right)} \qquad 3.20$$

5. When γ=10, then

$$0.01 = y_0 + \frac{a}{1 + \exp\left(\frac{x_0 - 1}{b}\right)} \qquad 3.21$$

The command line, In FLAC ^{3D}, for invoking these models requires that 4 symbols, *a*, *b* and x_0, and $y_0$are defined by the parameters ***v1***, ***v2***, and ***v3***, and ***v4***, respectively .Numerical fit for the curve of shear modulus reduction function given in equations 3.18,3.19,3.20,3.21 above solved simultaneously brings the values of 1.13071,-0.66217,-3.21549 and -0.0567 respectively.

3.3 Validation of the model

Here in this sub section the validation of what have been done so fare is made and hence the calibration of the laboratories results made by Boominathan And Tlakshm were performed . Accordingly, the tests result performed in a carefully designed small-scale pile test facility at the soil dynamics laboratory of IIT Madras was taken as guidance. This facility involves a masonry tank of inner dimensions of 2m x 2m x 1.5m. Elastic Half Space is simulated in the tank to obtain minimum reflection and maximum absorption of the waves generated during the vertical vibration. The elastic half space is simulated in the tank as shown in the Figure 3.7

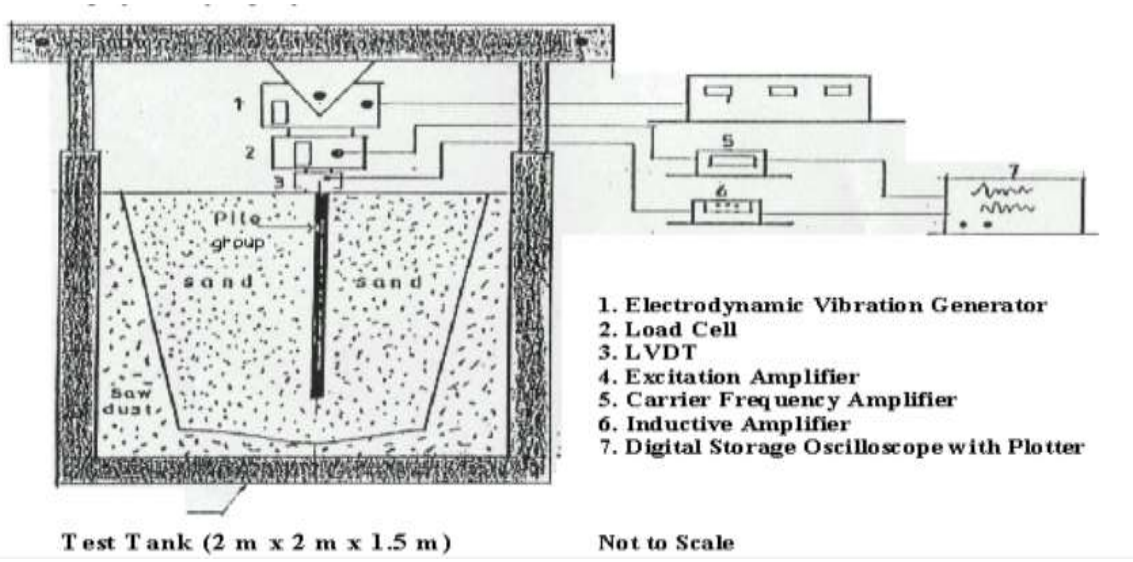

Figure 3.7 Vertical Vibration Test Setup

While numerical modeling is performed, therefore, the dimension of the soil, pile and that of pile cap was encoded in FDM software called FLAC ^{3D}.

3.3.1 Materials used while this test is performed

The test used Aluminum model piles of 19 mm outside diameter with a thickness of 2 mm for conducting the vertical vibration tests. Tests were conducted on single piles and on 2 x 2 and 3 x 3 pile groups. Pile caps made up of aluminum plate of size 130 mm x 130 mm x 20 mm in case of 2 x 2 groups, and of size 250 mm x 250 mm x 20 mm in case of 3 x 3 groups were used. Hence for this research a pile group of 2 x 2 is used in numerical simulation and intended to capture the results to compare with what was done in laboratory.

3.3.2 Test Procedure

While this test were performed, Steady state sinusoidal vertical excitations with very small amplitudes (4N - 10N) but high frequencies (5Hz-250Hz) were given at the pile head level by means of an Electro dynamic exciter. *HBM* strain gauge load cell was connected between the exciter and the pile head to determine the load transferred to the pile head. LVDT of *HBM* type was fixed to the pile head to measure the displacement of the pile head. The result of displacement of pile head with this much frequency gap was recorded and drawn as in figure 3.8 bellow. The normalized amplitude is calculated as

$$A = \frac{u}{F_0}$$

Where, u is the measured vertical displacement amplitude, F_0 is the applied force amplitude. The occurrence of a distinguished single peak in the response curves indicate that the system behaves as a damped single degree of freedom system within the range of frequencies considered.

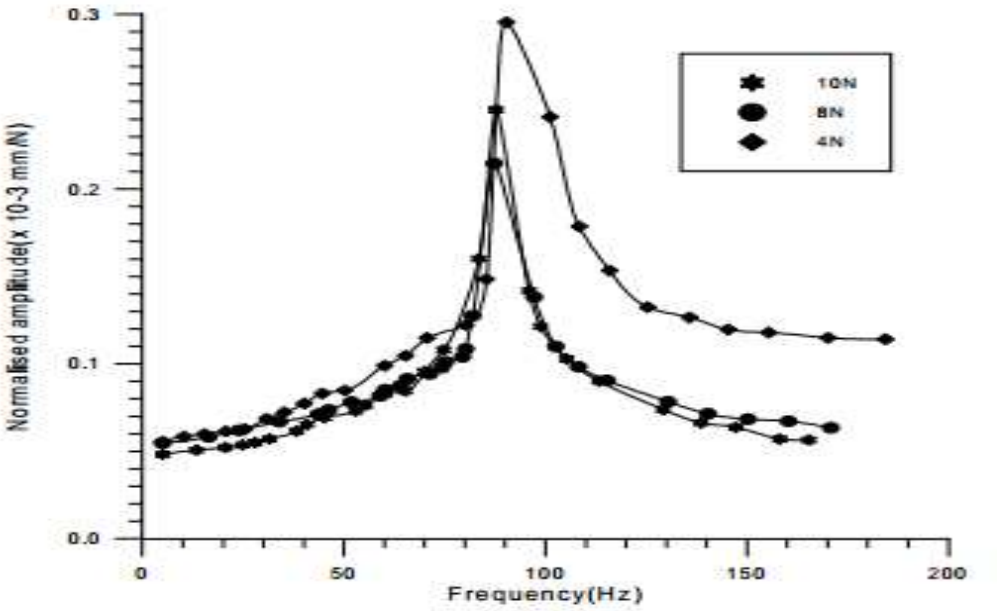

Figure 3.8 Normalized Amplitude as a function of frequency

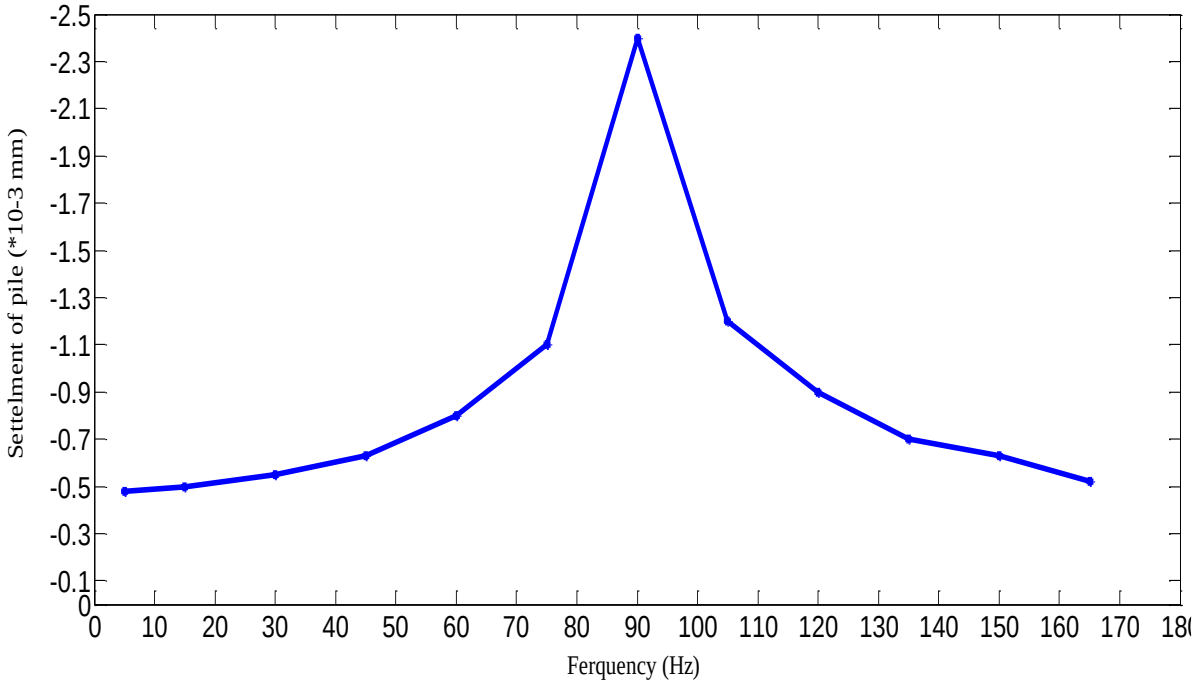

Figure 3.9 Settlement of pile as a function of frequency (lab result)

3.3.3 Comparison of test Results with Numerical Predictions

In this sub section a, a group pile of 2 x 2 subjected to Steady state sinusoidal vertical excitations of 10 N with high frequencies (5Hz-250Hz) were taken and modeled with FLAC^{3D} and the results were compared as shown in figure 4.22 &4.23 bellow.

Table 3.5 Comparison between numerical model and test results.

Frequency (Hz)	Lab Result (10^{-3}mm)	Numerical result (10^{-3}mm)
5	0.48	0.54
15	0.5	0.53
30	0.55	0.62
45	0.63	0.85
60	0.8	0.91
75	1.1	1.34
90	2.4	2.72
105	1.2	1.38
120	0.9	1.21
135	0.7	0.91
150	0.63	0.85
165	0.52	0.54

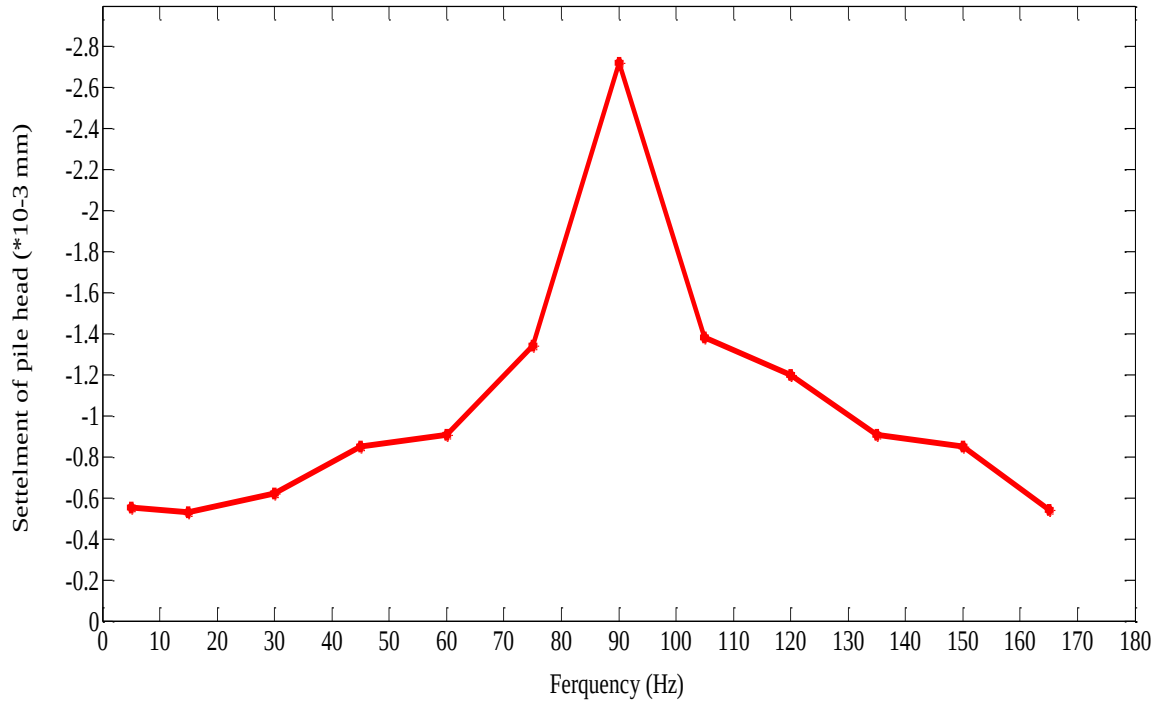

Figure 3.10 Settlement of pile head with dynamic excitation of 10 N (Numerical Result)

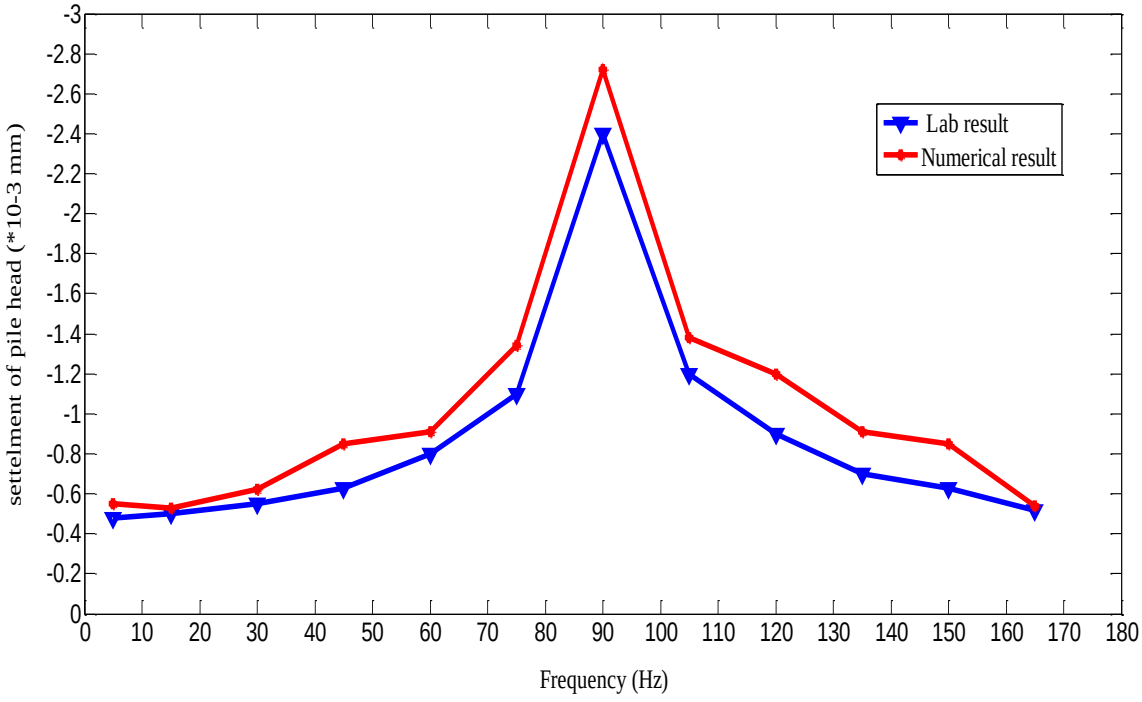

Figure 3.11 Comparison between numerical model and test result

4 RESULTS AND DISCUSSION

4.1 General

Parametric study is nothing but the investigation of the variation of solutions to the problem on the variation of different input parameters. In this research, therefore, a Parameter of Frequency of vibration of the dynamic load varies and ultimately the solutions were investigated. The solution were mainly settlement of the pile peak with in the variation of frequency loading. A single pile loaded dynamically at its center was taken for ease of analysis. Hence, the analysis of single pile settlement at the pile heads and finally the settlement of pile with variation of its length was investigated. The variation of axial load and side frictional load development was also studied and each of them were discussed briefly.

4.2 Numerical Pile Load

Numerical simulation of pile loading test was done. The pile was modeled using PILESEL command in FLAC^{3D} as attached in the appendix A of this document. The displacements at the pile head were captured using HISTORY command and the results are plotted.

In the following subsequent sub-sections the effect of frequency of vibration on single pile settlement was determined through numerical simulations. Table 4.1 summarizes the number of numerical analyses carried out in this section.

Table 4.1 The number of numerical analysis made with the corresponding frequency

Run#	D(m)	L/D	Frequency(Hz)
1	0.6	16.67	1
2	0.6	16.67	10
3	0.6	16.67	20
4	0.6	16.67	30
5	0.6	16.67	40

6	0.6	16.67	50
7	0.6	16.67	60
8	0.6	16.67	70
9	0.6	16.67	80
11	0.6	16.67	90

4.3 Initial Static conditions

The initial static condition of the soil pile interaction such as the initial displacements and stresses due to the weight of the superstructure and the soil should be considered before applying the seismic excitation was made. This results, however, rested to be zero in order to investigate the pure dynamic response and ultimately the total settlement of the pile was drawn since it is the sum of both static and dynamic settlement. The settlement of pile structure due to statically loading, whatever the variation of frequency is made or not, is constant (independent of frequency) because of the fact that the rearrangement of particles due to gravity is immense and beyond the duration of dynamic load.

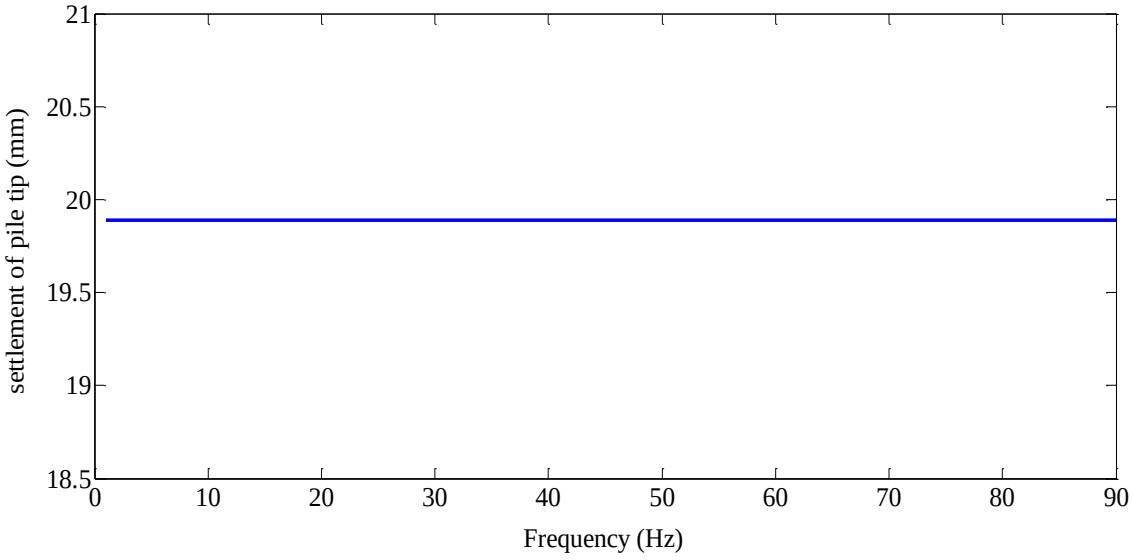

Figure 4.1Settlement of pile at initial static condition (constant, 19.98mm)

4.4 Response of pile for pure dynamic loading conditions

Here in this particular section it was intended to study the settlement of pile tip due to pure dynamic load and to do so the initial static conditions were rested to be zero and restored for further simulation for various frequencies and the results have been captured. From these settlement values it can be easily determined whether the individual pile was undergoing compressional or extensional deformation. The variation of pile settlement (combination of pile deformation, settlement due to variation of loading frequency) were presented in the subsequent table and interpreted accordingly.

Table 4.2 Settlement of pile head and tip at various frequencies of vibration

Frequency (Hz)	Pile head Displacement (mm)	Pile tip displacement (mm)
1	6.53	6.4
10	7.08	6.95
20	7.25	7.12
30	7.47	7.33
40	7.58	7.44
50	7.87	8.1
60	8.24	7.73
70	7.36	7.23
80	6.82	6.70
90	6.71	6.68

4.4.1 Displacement (settlement) of the pile at various frequency variation due to a single dynamic load

The settlement of the pile head at frequency variation was coded in FLAC ^{3D} and the out puts were monitored graphically as can be seen in the representative graph (figure 4.2) with deformation of pile head versus step of the calculation. From the graph it was possible to note that the deformation of the pile was minimum at the start of calculation and starts to increase until the equilibrium condition is attained and hence the corresponding settlement at equilibrium is considered as the settlement of the pile head with the corresponding frequency of vibration. And the variation of deformation with frequency was then plotted.

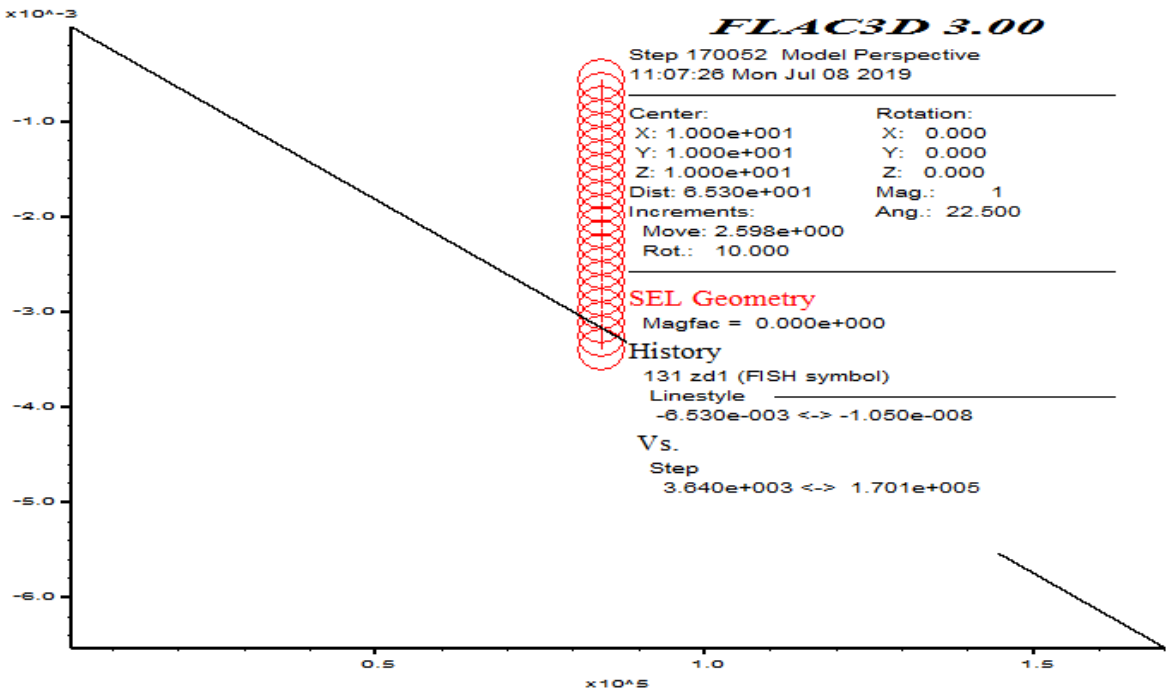

Figure 4.2 Displacement of pile Head with 1Hz vibrational loading

4.4.2 Displacement vs. frequency plots

The complex response of the system, ultimately, has the tendency to increase as frequency increases and after it has reached at a particular frequency it starts to decrease. This is so because faster loads cause smaller strains. The point of frequency at where the maximum deformation attained is the point of resonance at where the natural frequency of the soil-pile system and the frequency of loading are equal and it is the sever condition in dynamic analysis. In this particular research, therefore, the point where deformation of the pile become maximum is at 60 Hz frequency of vibration as can be shown in table 4.3 bellow.

Table 4.3 Variation of pile settlement with frequency

Frequency (Hz)	1	10	20	30	40	50	60	70	80	90
Pile settlement (mm)	6.53	7.08	7.25	7.47	7.58	7.87	8.24	7.36	6.82	6.71

The response of the system has investigated and found that it has the tendency to increase the settlement of the pile with increasing the frequency of loading up to a peak value of

deformation (settlement) and starts to decrease. The occurrence of this distinguished single peak in the response curves indicate that the system behaves as a damped single degree of freedom system within the range of frequencies considered. A point worth mentioning is the natural frequency of the soil-pile system in which the resonance of the system is developed, which the frequency is corresponding to the peak response. At this frequency of vibration the natural frequency of soil pile system and the frequency of loading are coincided and hence it is considered as sever condition. If, in case this frequencies are emanated simultaneously at a particular structure, it will be difficult to retain this structure. One can see that beyond this frequency the response of the pile is decreased (figure 4.12). This is so because faster loads cause smaller strains.

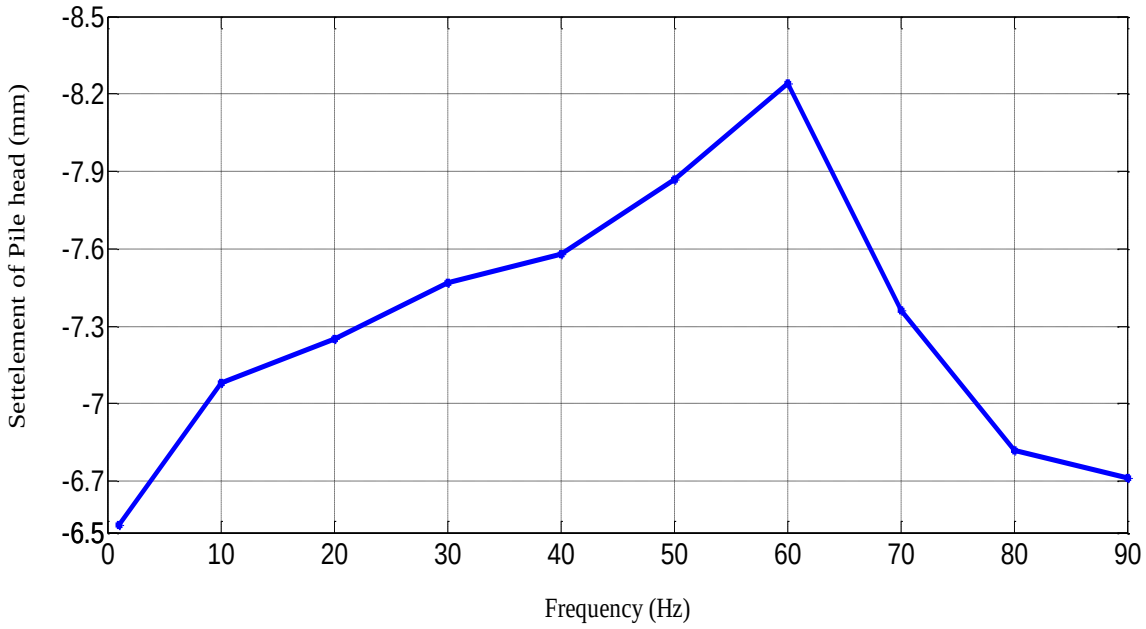

Figure 4.3 Settlement of pile head with varying Frequency

The response of the pile along with its length has been also investigated and found that it decreases as the length of the pile increases from the surface of the earth (figure 4.4), the negative sign indicates that the deformation is in the down ward direction.

Table 4.4 Showing settlement of pile along with its length with varying frequency

Settlement of pile (mm)										
Pile Length(m)	1 Hz	10 Hz	20 Hz	30 Hz	40 Hz	50 Hz	60 Hz	70 Hz	80 Hz	90 Hz
0	6.53	7.08	7.25	7.47	7.58	7.87	8.24	7.36	6.82	6.71
1	6.51	7.06	7.23	7.46	7.56	7.85	8.22	7.34	6.81	6.7
2	6.49	7.04	7.21	7.44	7.54	7.83	8.2	7.33	6.79	6.67
3	6.48	7.03	7.2	7.42	7.53	7.82	8.19	7.31	6.77	6.66
4	6.46	7.01	7.19	7.4	7.51	7.8	8.17	7.29	6.76	6.64
5	6.45	7	7.17	7.39	7.49	7.78	8.15	7.28	6.74	6.63
6	6.44	6.98	7.16	7.38	7.48	7.77	8.14	7.27	6.73	6.61
7	6.42	6.98	7.15	7.36	7.47	7.76	8.13	7.26	6.72	6.60
8	6.42	6.97	7.14	7.35	7.46	7.75	8.11	7.25	6.7	6.59
9	6.41	6.96	7.13	7.34	7.45	7.74	8.11	7.24	6.7	6.59
10	6.4	6.95	7.12	7.33	7.44	7.73	8.1	7.23	6.7	6.58

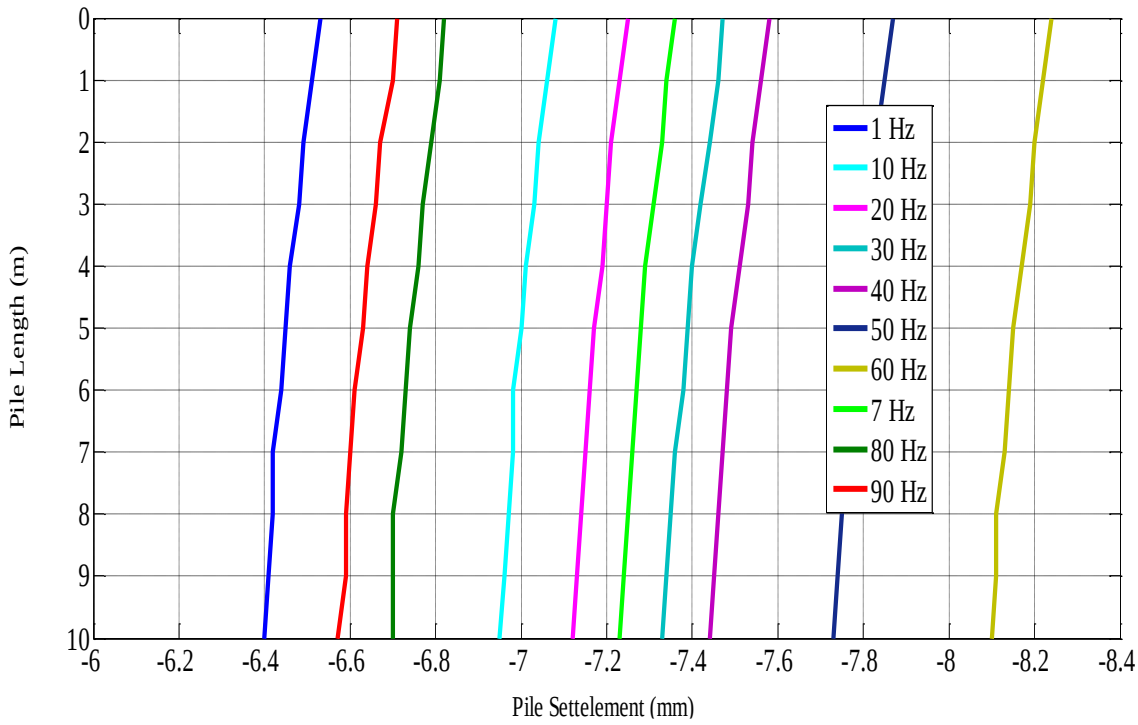

Figure 4.4 Settlement of pile corresponding with the length of the pile

4.4.3 Distribution of Friction Stress

The distribution of friction stress of the pile was also studied and the result can be shown in figure 4.5 bellow, which varies over frequency of vibration at a fixed dynamic time. The distribution and the values of pile side friction forces change over the period of vibration. The maximum point is the position in which the pile side friction changes. Hence at this point the pile side friction reach at peak value and starts to decrease which is correspondence with the 60 Hz frequency of vibration. It was declared that this frequency is also the one at which the maximum deformation is recorded. The Variation of frictional load through the length of the pile is also investigated and found that from the top to the bottom of pile, the algebraic value of the friction force is increasing, and the upper part of pile bears the minimum friction force, which gradually transforms into maximum friction force along the pile as tabulated in table 4.5.The maximum value of the positive friction force is obtained at the bottom of the pile.

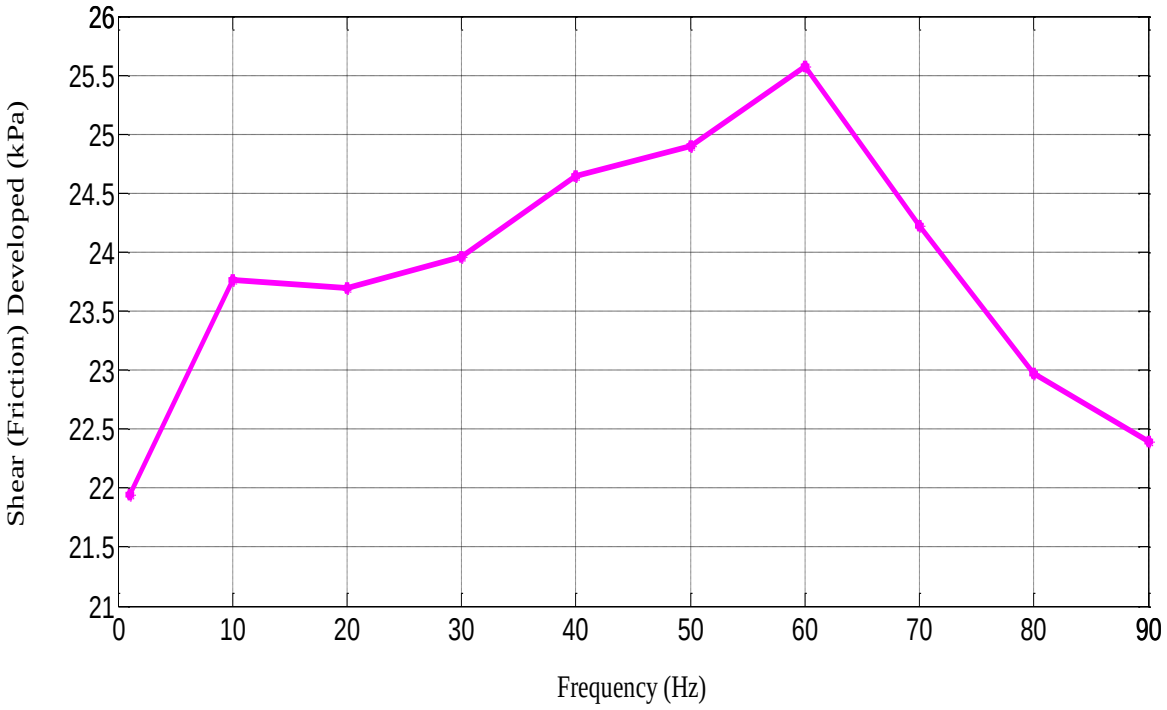

Figure 4.5 Pile side friction force variations with period of vibration

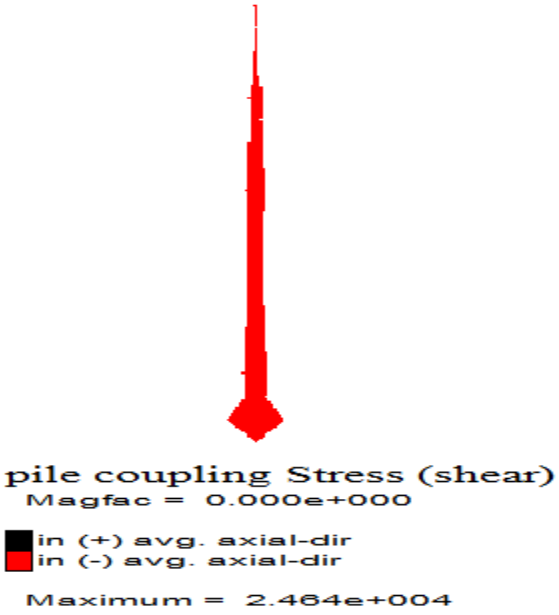

Figure 4.6 Pile side friction force along the pile depth (40 Hz).

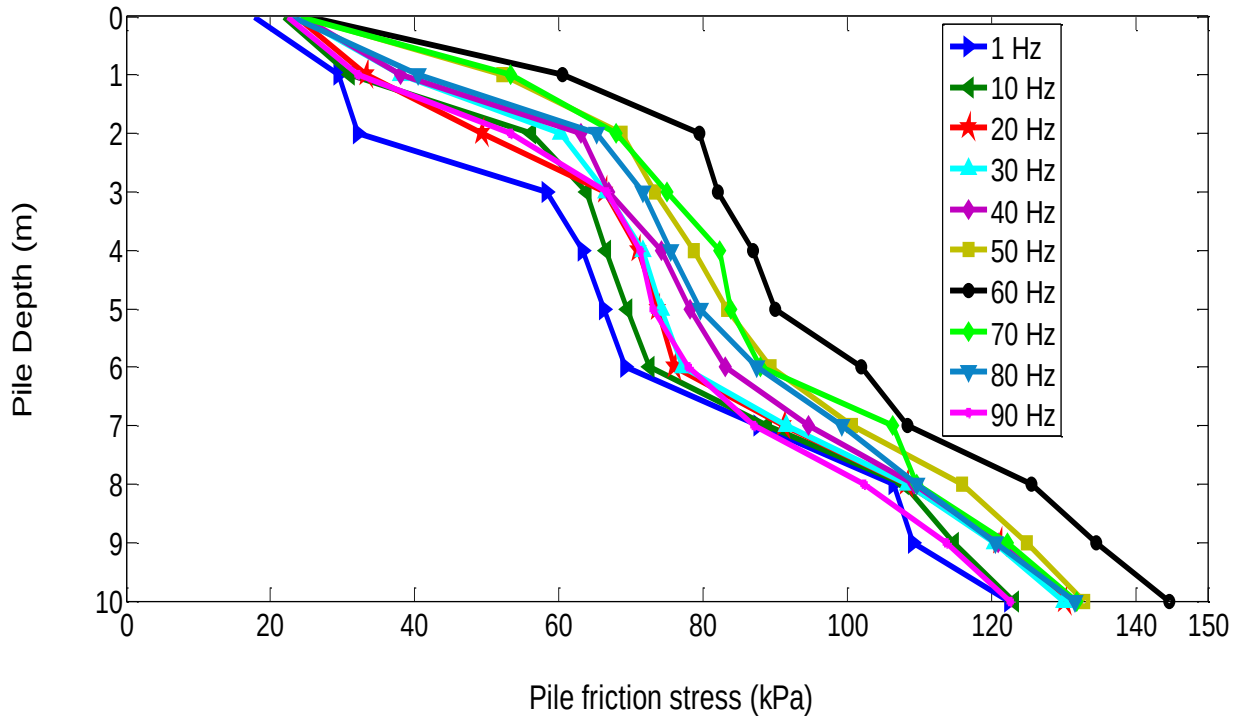

Figure 4.7 Pile side friction force variations along pile depth.

4.4.4 Distribution of Axial Force

For piles which are embedded in clay soil the neutral point will be just below the pile head and hence produce negative friction force above the neutral point and bears positive bellow this point (Boominathan A. and Ayothiraman R., 2006). In such case, above the neutral point, the pile bears the negative friction force and the axial force is the sum of its own weight and the negative friction force. Therefore, the axial force increases from the top of the pile to the neutral point. Below the neutral point, the pile bears the positive friction force and the axial force is the difference of its weight and the positive friction force. The axial force decreases gradually along the pile.in this research, however, the type of soil which the pile have been embedded is sandy soil so that there is no negative friction force development and hence the neutral point is purely somewhere out of the length of the pile. Consequently the friction force developed along with the pile length is purely positive and hence the sum of its own weight and positive friction force starts to decrease throughout the pile length as shown in the table 4.5 bellow.

Table 4.5 Variation of axial force within the length of the pile

Axial Force distribution (kN)										
Pile Length(m)	1 Hz	10 Hz	20 Hz	30 Hz	40 Hz	50 Hz	60 Hz	70 Hz	80 Hz	90 Hz
0	156.5	153.9	153.9	149.5	146.4	143	141.6	142.9	150.6	154.6
1	155.7	152.8	150.7	149.3	143.4	141.7	140.9	141.6	150.2	153.8
2	152.4	151	150.2	144.9	140.3	140.2	136.3	139.8	147.2	151.8
3	149.5	146.7	144.8	137.5	134.9	135.5	130.2	134.9	140.9	148.1
4	136.7	134.9	132.9	128	120.1	129.1	119.5	123.8	131.5	136.6
5	127.5	123	121.1	117.4	119.6	113.4	110.4	111.3	121.8	123
6	118.8	112.7	112.3	109.9	104.2	106.9	103.9	106	110.6	112.3
7	106.5	102.6	101.2	97.75	94.58	95.75	92.82	94.74	99.47	103.6
8	99.24	90.6	88.11	85.89	80.64	84.3	80.8	83.13	84.6	91.00
9	77.83	74	71.6	70.22	66.7	69.2	62.58	66.78	68.85	74.58
10	51.25	49.07	48.99	48	47.43	46.68	41.9	45.78	46.97	50.78

The axial force distribution of the pile head decreased with increasing frequency of vibration and returns back to increase. Figure 4.8 bellow shows the variation of pile axial force over period of vibration at a particular dynamic time. The position where this change of axial force developed is correspondence with the frequency of 60 Hz. With respect to pile depth variation it is found that from the top to the bottom of the pile, the axial force of pile decreases along the pile shaft which is the reverse of pile side friction. Figure 4.9 and 4.10 show the variation of pile axial force variation with respect to the pile depth. In addition, the maximum value is obtained at the pile head, at which the friction force is minimum.

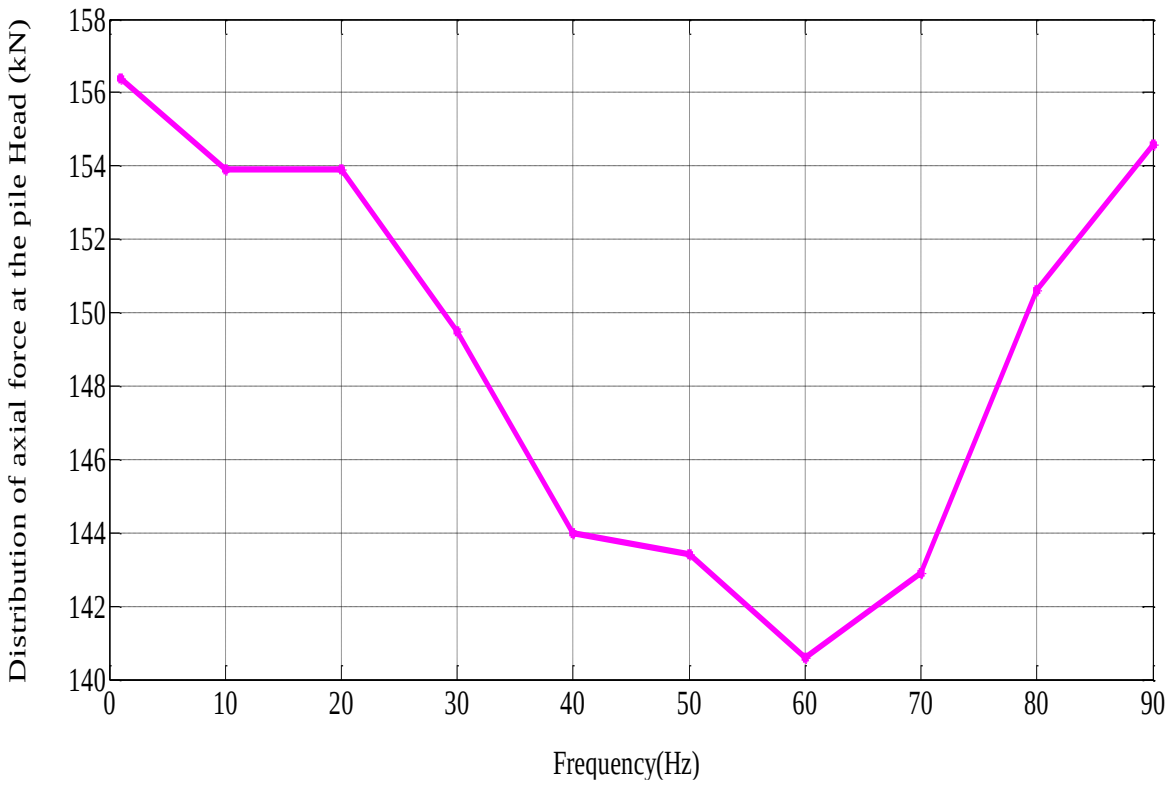

Figure 4.8 Distribution of axial force at the peak of the pile (Pile head)

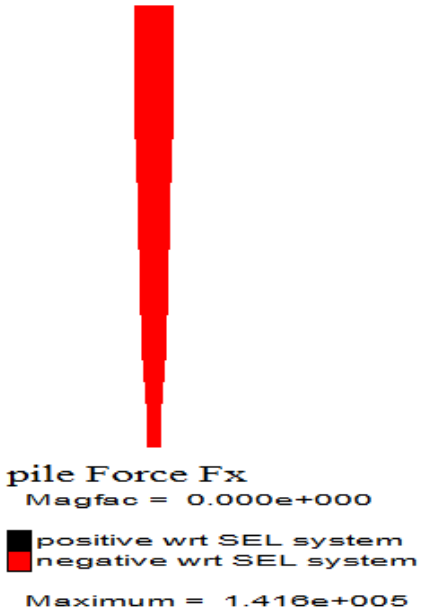

Figure 4.9 Distribution of the pile axial force over the pile depth

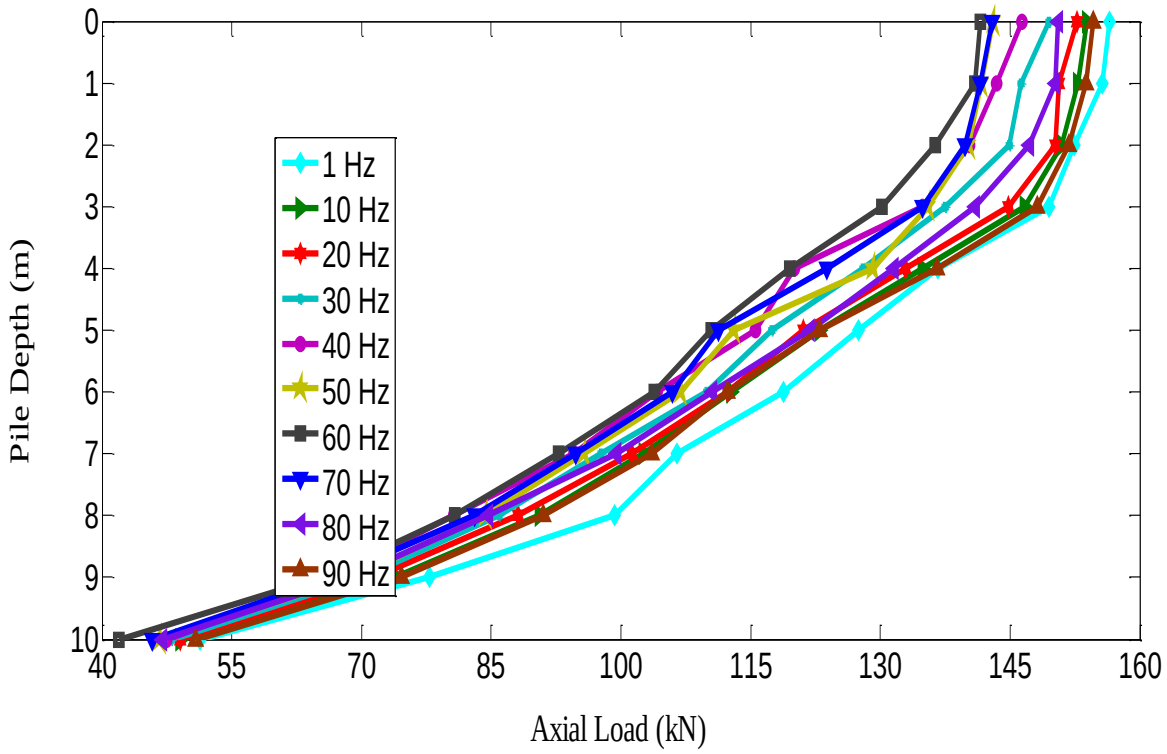

Figure 4.10 Pile Axial force variations along pile depth.

4.4.5 Displacement Contours of the Soil around Pile.

Figure 4.11 shows the numerical displacement contour of the soil around pile at a particular frequency of 60 Hz, in which the negative value indicates the downward direction of the displacement. Considering the impact of the pile side friction force, the soil is propped up and down by the pile. However, given the effect of seismic loads especially the longitudinal waves, the settlement of soil changes significantly. But the variation rule is not monotonous. The compression and stretching effects on the soil occur alternately when the longitudinal waves pass. Consequently, the soil settlement increases and decreases alternately while the process of calculation is executed. The settlement, however, reaches its maximum value of 8.24 mm when the seismic duration reach targeted dynamic time of 2.5sec.

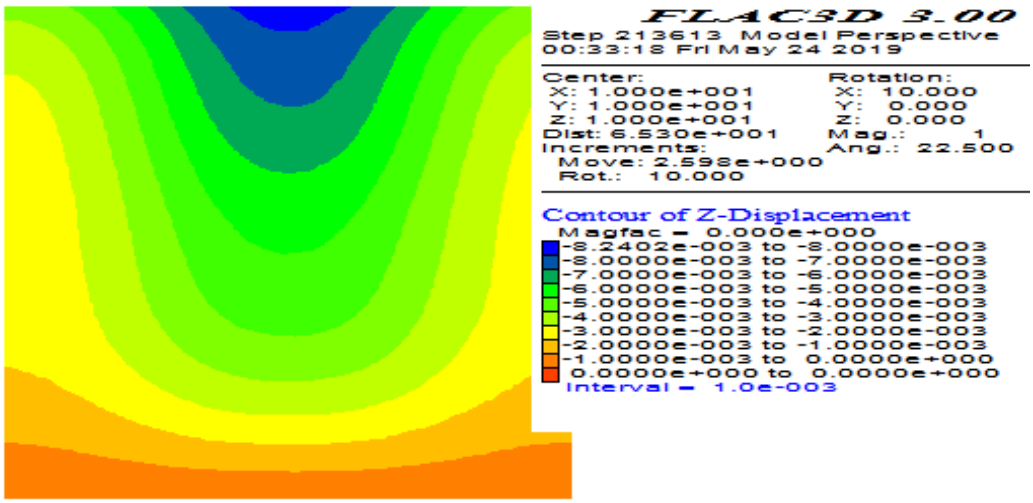

Figure 4.11 Vertical displacement contour of the soil around pile under 60 Hz frequency of vibration.

4.5 Total settlement (Displacement) of pile

The settlement (deformation) of the pile ultimately is such that the sum of both the result of static and that of dynamic loading conditions and hence was elaborated in a comparison form as shown in the figure 4.12 bellow.

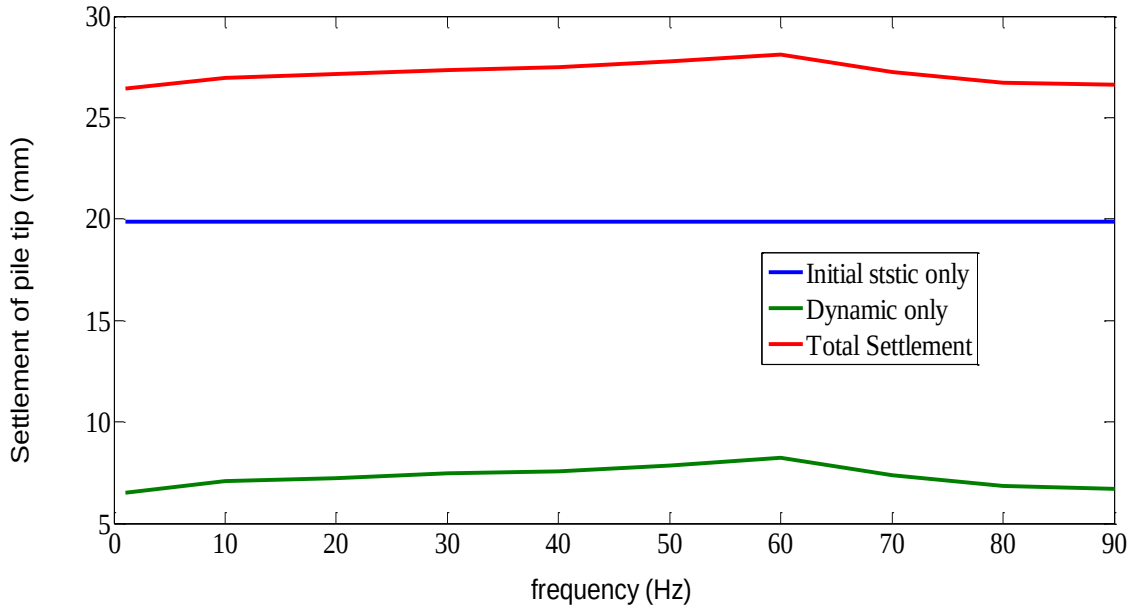

Figure 4.12 Comparison of settlement of pile tip for both loading condition

5 CONCLUSIONS AND RECOMMENDATIONS

5.1 Conclusions

Structural behaviour is inherently nonlinear, particularly in the presence of large displacements or material nonlinearities, the structural response can be accurately caught only by means of nonlinear dynamic analyses. The finite difference method modelling approach employed in the current work is shown to be capable of grasping the soil non linearity. Moreover, its ability to simulate the nonlinear dynamic response of underground structures to seismic loads has been proven by simulating the results of large-scale experimental tests. After wards In accordance with the discussions made so far, the analysis results obtained from FLAC^{3D} are discussed and relevant comparisons of the results obtained using FLAC ^{3D} with the available laboratorically results obtained are made. Hence, the following conclusions are drawn:

1. In the results, it was seen that generally the response, settlement of pile, has a tendency to increase with frequency up to some value of frequency, which is called as point of resonance, and further increase of frequency results the decrement of response (settlement) of pile. This is so because faster loads induce smaller response.
2. The interaction between the pile and soil consists of two components, one normal to the surfaces and one tangential to the surfaces. The tangential component consists of the relative motion (sliding) of the surfaces and, possibly, frictional shear stresses. The surfaces separate when the contact pressure between them becomes zero or negative. This behavior, referred to as “hard” contact which is mainly the Characterstics of cohesive soil. Whereas if the frictional shear stress are positive, then the contacting condition is said to be smooth contact which is the characteristics of chohesionless soil. Since while a pile is subjected to dynamic load, it is necessary to check that the soil which it intended to embed is chohesionless soil in such a way that the contact between the soil and pile is smooth as discussed so far.
3. The axial force and frictional stress distribution with the pile length has discussed and concluded that the axial force distribution decreases with pile length and vice versa was found with frictional stress. This is so because as the length of the pile

increased the contacting area in between the soil and the pile is increased and vice versa is true for axial force.

4. Also the variation of axial force and frictional stress with the frequency of vibration were made and came up with the conclusion that the axial force distribution decreases with frequency up to point of resonance and starts to increase. This is so because high vibration increases the motion between the soil and the pile which increases friction in between them which is called as the friction stress and hence most of the loads are resisted by friction than axial and the axial force distribution with the pile length decrease with frequency. The distribution of axial load and friction stress with frequency, therefore, are reversed.
5. While the design of pile subjected to dynamic load, it is necessary that the natural frequency of the system has to be determined. Because it is important to design structures in such a way that the frequencies at which they may be loaded are not close to the natural frequencies and if the loading condition of a pile is exactly with the natural frequency, the failure mechanism is sever.
6. If the pile is driven into consolidated soil and the settlement of the pile is greater than that of the soil, the pile is supported by the soil, and positive friction force is produced. If the settlement of the soil, however, is greater than that of the pile, the pile is pulled down by the soil, and negative friction force is produced. Given the pulling effect of soil, the negative friction force on the pile side will reduce its carrying capacity, causing engineering instability which is observed in this thesis. So piles subjected to dynamic load, whether it is single or double, the probability of development of negative pile side friction is high due to periodic loading and hence care should be taken while designing piles prone to dynamic area is made.

5.2 Recommendations

Dynamic analysis of a soil-pile system is a vast field which needs plenty time and effort when a comprehensive analysis is sought. In this Master's thesis, therefore, the focus has been prediction of the vertical displacement of single pile subjected to dynamic load inducing large strains, i.e. nonlinear analysis. Due to the vastness of analysis, this thesis is limited to only the variation parameter to be frequency of vibration only and the soil strata a pile to be embedded in is homogeneous. Hence needs to recommend on points for further researchers.so the following recommendations are drawn for future research.

1. In this thesis, the analysis is limited to a homogeneous soil of sand , but in practical the pile to be embedded may not be purely homogeneous and piles embedded in stratified soil subjected to dynamic load is recommended to be studied.
2. Practically, a pile might be subjected to different actions even though the predominant type of loading is an axial. There are occasions when a lateral load can be considerable in a structure located in areas where earthquake or wind loads are prominent. Hence the analysis of pile subjected to lateral dynamic load needs to be studied.
3. This thesis was tried to investigate the effect of dynamic load on a single pile. Practically, however, installing a single pile as a foundation is rare and pile groups instead are applicable. Hence pile group analysis subjected to dynamic load is recommended for further study.
4. Also in this thesis, the response of a pile subjected to a single dynamic load for a short period of time (2.5 sec dynamic time) has been investigated due to the vastness of modeling and for further researchers, the author of this research wants to recommend that the response of pile foundations by varying the intensity of load and extending the duration of it has to be take in to account.

REFERENCES

Adimoolam et al. (2013). Dynamic Response of Piles ─ Case Studies in India. *International Conference on Case Histories in Geotechnical Engineering.* Askar.

Ali Gandomzadeh et al. (2008). a simplified non-linear spring approach for dynamic soil-structure interaction. *the 14th World Conference on Earthquake Engineering.* Beijing, China.

Alian pecker. (2007). *Advanced Earth quake Engineering Analysis.* Newyork: SpringerWein.

ANSYS. (2005). *ANSYS Training Manual.*

Boominathan A. and Ayothiraman R. (2006). Dynamic response of laterally loaded piles in clay. *Geotechnical Engineering Journal, ICE-UK,*, 159[3] 233–241.

Bowles. (1996). *"Foundation Analysis and Design" 4th Ed.* New York, 308.: the McGraw-Hill Companies, Inc.

Bowles, Joseph E. (1996). *Foundation Analysis and Design,5 th ed.* Singapore: McGraw-Hill Companies,Inc.

Braja M. Das, G.V. Ramana. (2011). *Principles of Soil Dynamics, Second.* stamford,USA.

Cernica, J. N. (1995). *Geotechnical Engineering: Foundation Design.* New York : John Wiley & Sons, Inc.

Chong, Song-Hun. (2017). Soil Dynamic Constitutive Model for Characterizing the Nonlinear-Hysteretic Response. *High Speed Railroad Systems Research Center, Korea Railroad Research Institute, 176, Cheoldo bangmulgwan-ro, Uiwang-si, Gyeonggi-do*, 437-757.

CSI. (2009). *Analysis Reference manual.* California: University of avenue.

Darendeli, M. (2001). *Development of a New Family of Normalized Modulus Reduction and Material Damping Curves. Ph.D. Thesis, University of Texas at Austin.* Austin, TX, USA.

EBCS. (2013). *Design of Structures for Earthquake Resistance.* Addis Ababa, Ethiopia: Ministry of Urban Development & Construction.

Fekadu, P. (2010). *"Simulating the dynamic response of a Soil-Pile system using ABAQUS" thesis presented to CHALMERS UNIVERSITY OF TECHNOLOGY.* Goteborg, Sweden.

Gandomzadeh, A. (2011). *"Dynamic soil-structure interaction : effect of nonlinear soil behavior''thesis submitted to Universit´e Paris Es, Ecole Doctorale : ´ SIE - Sciences, Ing´enierie et Environment, Sp´ecialit´e : G´eotechnique.*

Hartzell, S. et al. (2004). Prediction of Nonlinear Soil Effects. *Bull. Seismol. Soc. Am*, 94, 1609–1629.

Hashash, Y.M.A. Park,D. (2002). Viscous damping formulation and high frequency motion propagation in non-linear site response analysis. *Soil Dyn. Earthq. Eng.*, 22, 611–624.

Itasca. (2012). *Fast Lagrangian Analysis of Continua in 3 Dimensions, User Manual, Second Edition (FLAC3D Version 3.0).* Minneapolis, Minn, USA,: Itasca Consulting Group.

Kim et al. (2013). *Centrifuge test for seismic load of structure affected by soft soil deposit.* KAIST, Daejeon,Korea.: Construction Technology Innovation Program funded by Ministry of Land, Transport and Maritime Affairs of Korean government.

Kuhlemeyer et al. (2010). Finite Element Method Accuracy for Wave Propagation Problems. *Soil Mech. & Foundations, Div. ASCE, 99(SM5)*, 421-427.

Mamo, B. (2016.). *"Three dimensional numerical investigations on the behavior of pile group in sand for vertical loading" Thesis presented to School of graduate Studies, Bahir Dar University, Civil Engineering Department.* Bahir dar,Ethiopia.

Meyerhof, G. G. (1976). Bearing capacity and settlement of pile foundations. *J. Geotech. Eng'g. Div., ASCE,*, 102(3), 195–228.

Mohammad M . Ahmedin and Mahdi Ehsan. (2008). Dynamic analysis of piles in sand based on soil-pile interaction. *The 14th World Conference on Earthquake Engineering.* Beijing, China.

Nogami and Konagai. (1987). Dynamic Response of Vertically Loaded nonlinear Pile foundations. *Journal of Geotechnical Engineering, ASCE,*, Vol. 113, No. 2.

Nogami et al. (1991). Seismic Response Analysis of Pile-Supported Structure: Assessment of Commonly Used Approximations. *Nogami, Toyoaki; Mosher, Reed L.; and Jones, H. Wayne, "Seismic Response Analysis of Pile-Supported Structure: A International Conferences on Recent Advances in Geotechnical Earthquake Engineering and Soil.* USA: Scholars' Mine.

Nogami, and Konagai. (1987). Dynamic Response of Vertically Loaded nonlinear Pile foundations. *Journal of Geotechnical Engineering, ASCE,*, Vol. 113, No. 2.

Novak, M. (1985). "Experiments with shallow and deep foundations", In Vibration Problems in Geotechnical Engineering. *Eds. Gazetas, G. and Selig, E. T.*, , 1-26.

Rini Kusumawardani et al. (2015). Cyclic Shear Strain Threshold on Clean Sand due to Cyclic Loading. *International Journal of Innovative Research in Science.* Indonesia: Engineering and Technolog Soil Mecahnics Laboratory, Dept. of Civil Engineering, Universitas Negeri Semarang.

Ronaldo I. Borja. (2000). *"Modelling non-linear ground response of non-liquefiable soils".* U.S.A: Department of Civil and Environmental Engineering, Stanford UniversityStanford University, Stanford, CA 94305-4020.

Wood, d. M. (1990). *Soil Behavioure and Critical state Soil mechanics.* New york, USA: Cambridge University press.

APPENDIX A: SAMPLE CODE FILES

Table A.1Code file developed to create the geometry of the block and initial stresses within the soil.

```
new
conf dynamic
set dynamic=off
gen zone brick p0 0 0 0 p1 8 0 0 p2 0 8 0 p3 0 0 10 p4 8 8 0 p5 0 8 10 p6 8 0 10 &
                p7 8 8 10 size 16 16 20 group Sand
gen zone brick p0 0 0 10 p1 8 0 10 p2 0 8 10 p3 0 0 20 p4 8 8 10 p5 0 8 20 p6 8 0 20 &
                p7 8 8 20 size 16 16 20 group Sand
gen zone brick p0 12 0 0 p1 20 0 0 p2 12 8 0 p3 12 0 10 p4 20 8 0 p5 12 8 10 p6 20 0 10 &
                p7 20 8 10 size 16 16 20 group Sand
gen zone brick p0 12 0 10 p1 20 0 10 p2 12 8 10 p3 12 0 20 p4 20 8 10 p5 12 8 20 p6 20 0 20 &
                p7 20 8 20 size 16 16 20 group Sand
gen zone brick p0 0 12 0 p1 8 12 0 p2 0 20 0 p3 0 12 10 p4 8 20 0 p5 0 20 10 p6 8 12 10 &
                p7 8 20 10 size 16 16 20 group Sand
gen zone brick p0 0 12 10 p1 8 12 10 p2 0 20 10 p3 0 12 20 p4 8 20 10 p5 0 20 20 p6 8 12 20 &
                p7 8 20 20 size 16 16 20 group Sand
gen zone brick p0 12 12 0 p1 20 12 0 p2 12 20 0 p3 12 12 10 p4 20 20 0 p5 12 20 10 &
                p6 20 12 10 p7 20 20 10 size 16 16 20 group Sand
gen zone brick p0 12 12 10 p1 20 12 10 p2 12 20 10 p3 12 12 20 p4 20 20 10 p5 12 20 20 &
                p6 20 12 20  p7 20 20 20 size 16 16 20 group Sand
gen zone brick p0 8 0 0 p1 12 0 0 p2 8 8 0 p3 8 0 10  p4 12 8 0 p5 8 8 10  p6 12 0 10 &
                p7 12 8 10 size 16 16 20 group Sand..... to be continued on next page
```

```
gen zone brick p0 8 0 10 p1 12 0 10 p2 8 8 10 p3 8 0 20  p4 12 8 10 p5 8 8 20  p6 12 0 20&
                p7 12 8 20 size 16 16 20 group Sand
gen zone brick p0 8 12 0 p1 12 12 0 p2 8 20 0 p3 8 12 10  p4 12 20 0 p5 8 20 10  p6 12 12 10 &
                p7 12 20 10 size 16 16 20 group Sand
gen zone brick p0 8 12 10 p1 12 12 10 p2 8 20 10 p3 8 12 20  p4 12 20 10 p5 8 20 20  &
                 p6 12 12 20  p7 12 20 20 size 16 16 20 group Sand
gen zone brick p0 0 8 0 p1 8 8 0 p2 0 12 0 p3 0 8 10 p4 8 12 0 p5 0 12 10 p6 8 8 10 &
                 p7 8 12 10 size 16 16 20 group Sand
gen zone brick p0 0 8 10 p1 8 8 10 p2 0 12 10 p3 0 8 20 p4 8 12 10 p5 0 12 20 p6 8 8 20 &
                p7 8 12 20 size 16 16 20 group Sand
gen zone brick p0 12 8 0 p1 20 8 0 p2 12 12 0 p3 12 8 10 p4 20 12 0 p5 12 12 10 p6 20 8 10 &
                p7 20 12 10 size 16 16 20 group Sand
gen zone brick p0 12 8 10 p1 20 8 10 p2 12 12 10 p3 12 8 20 p4 20 12 10 p5 12 12 20 &
                p6 20 8 20 p7 20 12 20 size 16 16 20 group Sand
gen zone brick p0 8 8 0 p1 12 8 0 p2 8 12 0 p3 8 8 10 p4 12 12 0 p5 8 12 10 p6 12 8 10 &
                 p7 12 12 10 size 16 16 20 group Sand
gen zone brick p0 8 8 10 p1 12 8 10 p2 8 12 10 p3 8 8 20 p4 12 12 10 p5 8 12 20 p6 12 8 20 &
                p7 12 12 20 size 16 16 20 group Sand
;=================================================
; Constitutive Model for Sand
Model mohr range group sand
prop bulk=62.267e6 shear=37.36e6 fric 43 coh 0 dens 1550.46   range group sand
;Boundary conditions
fix z range z=(-0.1,0.1)
fix x range x=(-0.1,0.1)
fix x range x=(19.9,20.1)
fix y range y=(-0.1,0.1)
fix y range y=(19.9,20.1)
set grav=0,0,-10 larg
plot show base
solve
```

Table A.2 Code file developed to install the pile in soil block and mechanical analysis.

```
;Create a pile  in the center of the sand block
;============================
sel pile id=1 begin=10 10 20 end=10 10 10 nseg=20

sel pile prop Emod=3.0e10 Nu=0.25 XCArea=0.2826 XCJ=1.21e-3 XCIy=6.36e-3 XCIz=6.36e-3 slide on range z 10 20

sel pile prop per=1.884955

sel pile prop CS_sK=6.67e11 CS_sCoh=0.0 CS_sFric=43.0  slide on range z 10 20

sel pile prop CS_nK=6.67e11 CS_nCoh=0 CS_nFric= 0.0 CS_nGap=off slide on range z 10 20

sel pile prop slide on range z 10 20

sel pile prop dens 2548

plot add sel geom red

;end bearing effect

sel delete link range id 21

sel link id=100 2 target zone

sel link attach ydir=free zdir=free range id 100

sel link attach xrdir=free yrdir=free zrdir=free range id 100

sel link attach xdir=nydeform range id 100

sel link constit nydeform 1 area=1 k=6.67e11 ycomp=3.59e5 range id 100

save pile instalation.save

solve

save pile mech-29-6-11
;============================================
```

Table A.3 Code file used to include the dynamic loading condition using the mechanical one as initial.

```
;dynamic part
set dynamic=on large
restore pile mech-29-6-11
ini xdis=0 ydis=0 zdis=0 xv=0 yv=0 zv=0
plot show
def stiff_var
pnt= zone_head
   loop while pnt # null
      sgm_m=79e3; minimum effective stress of 79kPa is used to avoid sqrt of negative
nmber and excessive mesh distortion
              ; this is equivalent to depth of about 5m(at the mid of pile lenth) from pile head.
     if  z_group(pnt)='sand' then
        p_ratio=0.25
        sgm1=(z_sxx(pnt)+z_syy(pnt)+z_szz(pnt))/3+z_pp(pnt); sgm1- mean effective stress
        sgm=max(sgm1,sgm_m) gmax=53.38e6
      z_prop(pnt,'shear')=gmax; (pa)
      z_prop(pnt,'bulk')=(2.0*(1+p_ratio)/(3.0*(1-2*p_ratio)))*z_prop(pnt,'shear')
     end_if
pnt=z_next(pnt)
end_loop
end
stiff_var
;=============================================================
; Dynamic Loading
def setup
omega = 2.0 * pi * freq
pulse = 1.0 / freq
end
set freq=60
setup.....to be continued on next page
```

```
def wave
if dytime > pulse
wave = 0.0
else
wave = (1.0 - cos(omega * dytime)) / 2.0
endif
end
def Q
Q=(-10e3)*exp(omega*dytime)
end
sel node FIX x range id=1
apply Zforce = Q range id=1
setup

; Dynamic boundary conditions
;=============================================================
set dyn damp local 0.1571  ; = pi * 0.05 which is 5% local damping

;Hysteretic damping:  the sigmoidal hysteretic damping model with four parameters is used

initial damp hyst sig4  1.1307  -0.66217  -3.21549  -0.0567  range group sand

;history point; are the points interested to at the peak of the pile, 5m depth, 10m depth(at
the end of the pile),15m depth and 20m depth(at the end of the block) Respectively.
;=============================================================
```

Table A.4 Code file developed for monitoring points (history points)

```
def const
p_gp1 =      gp_near(10,10,20)
p_gp2 =      gp_near(10,10,19)
p_gp3 =      gp_near(10,10,18)
p_gp4 =      gp_near(10,10,17)
p_gp5 =      gp_near(10,10,16)
p_gp6 =      gp_near(10,10,15)
p_gp7 =      gp_near(10,10,14)
p_gp8 =      gp_near(10,10,13)
p_gp9 =      gp_near(10,10,12)
p_gp10       =      gp_near(10,10,11)
p_gp11       =      gp_near(10,10,10)
p_gp12       =      gp_near(10,10,9)
p_gp13       =      gp_near(10,10,8)
p_gp14       =      gp_near(10,10,7)
p_gp15       =      gp_near(10,10,6)
p_gp20       =      gp_near(10,10,0)
end
const
 def dispts
 dispts =    gp_xdisp(p_gp1)
xd1    =     gp_xdisp(p_gp1)
xd2    =     gp_xdisp(p_gp2)
xd3    =     gp_xdisp(p_gp3)
xd4    =     gp_xdisp(p_gp4)
xd5    =     gp_xdisp(p_gp5)
xd6    =     gp_xdisp(p_gp6) .....to be continued on next page
```

```
xd7    =      gp_xdisp(p_gp7)
xd8    =      gp_xdisp(p_gp8)
xd9    =      gp_xdisp(p_gp9)
xd10   =      gp_xdisp(p_gp10)
xd11   =      gp_xdisp(p_gp11)
xd12   =      gp_xdisp(p_gp12)
xd13   =      gp_xdisp(p_gp13)
xd14   =      gp_xdisp(p_gp14)
xd15   =      gp_xdisp(p_gp15)
xd20   =      gp_xdisp(p_gp20)
;y_displacements
yd1    =      gp_ydisp(p_gp1)
yd2    =      gp_ydisp(p_gp2)
yd3    =      gp_ydisp(p_gp3)
yd4    =      gp_ydisp(p_gp4)
yd5    =      gp_ydisp(p_gp5)
yd6    =      gp_ydisp(p_gp6)
yd7    =      gp_ydisp(p_gp7)
yd8    =      gp_ydisp(p_gp8)
yd9    =      gp_ydisp(p_gp9)
yd10   =      gp_ydisp(p_gp10)
yd11   =      gp_ydisp(p_gp11)
yd12   =      gp_ydisp(p_gp12)
yd13   =      gp_ydisp(p_gp13)
yd14   =      gp_ydisp(p_gp14)
yd15   =      gp_ydisp(p_gp15)
yd20   =      gp_ydisp(p_gp20) .....to be continued on next page
```

```
;Z_displacements
zd1     =       gp_zdisp(p_gp1)
zd2     =       gp_zdisp(p_gp2)
zd3     =       gp_zdisp(p_gp3)
zd4     =       gp_zdisp(p_gp4)
zd5     =       gp_zdisp(p_gp5)
zd6     =       gp_zdisp(p_gp6)
zd7     =       gp_zdisp(p_gp7)
zd8     =       gp_zdisp(p_gp8)
zd9     =       gp_zdisp(p_gp9)
zd10    =       gp_zdisp(p_gp10)
zd11    =       gp_zdisp(p_gp11)
zd12    =       gp_zdisp(p_gp12)
zd13    =       gp_zdisp(p_gp13)
zd14    =       gp_zdisp(p_gp14)
zd15    =       gp_zdisp(p_gp15)
zd20    =       gp_zdisp(p_gp20)
end
;histry of x_disp
his     id      101         xd1
his     id      102         xd2
his     id      103         xd3
his     id      104         xd4
his     id      105         xd5
```

.....to be continued on next page

```
his   id      106     xd6
his   id      107     xd7
his   id      108     xd8
his   id      109     xd9
his   id      110     xd10
his   id      111     xd11
his   id      112     xd12
his   id      113     xd13
his   id      114     xd14
his   id      115     xd15
;histry of y_displa
his   id      116     yd1
his   id      117     yd2
his   id      118     yd3
his   id      119     yd4
his   id      120     yd5
his   id      121     yd6
his   id      122     yd7
his   id      123     yd8
his   id      124     yd9
his   id      125     yd10
his   id      126     yd11
his   id      127     yd12
his   id      128     yd13
his   id      129     yd14
his   id      130     yd15.....
```

to be continued on next page

```
;histry of z_displa
his    id      131      zd1
his    id      132      zd2
his    id      133      zd3
his    id      134      zd4
his    id      135      zd5
his    id      136      zd6
his    id      137      zd7
his    id      138      zd8
his    id      139      zd9
his    id      140      zd10
his    id      141      zd11
his    id      142      zd12
his    id      163      zd13
his    id      144      zd14
his    id      145      zd15
his    id      146      zd20
set dyn multi on
solve age 2.5
save pile_f60date29_.sav


                ;THE END
        ;=============================================
```

APPENDIX B: REPRESENTATIVE RESPONSE AT 60 HZ FREQUENCY.

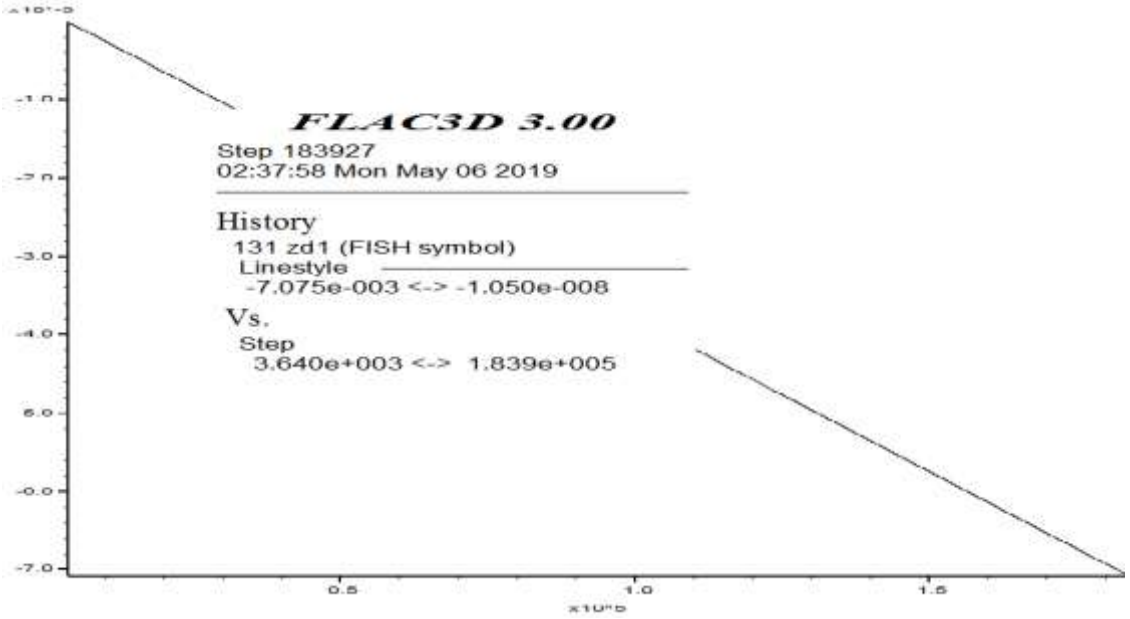

Figure B.1 Displacement of pile Head with 10 Hz vibrational loading

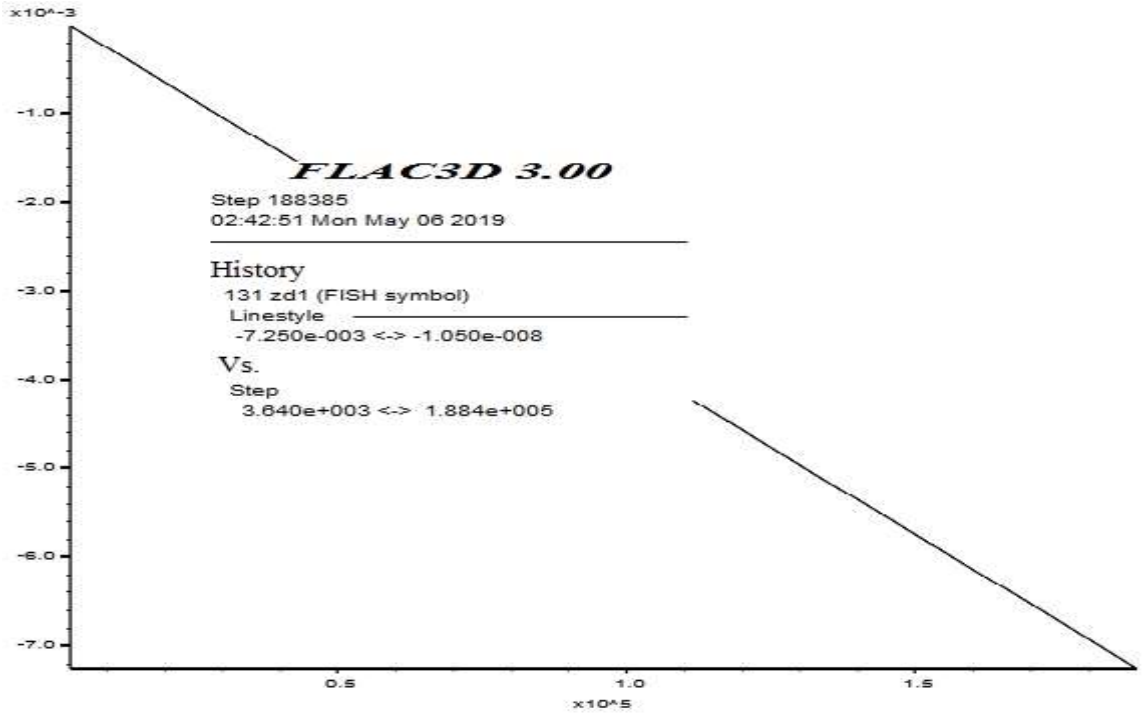

Figure B.2 Displacement of pile Head with 20 Hz vibrational loading

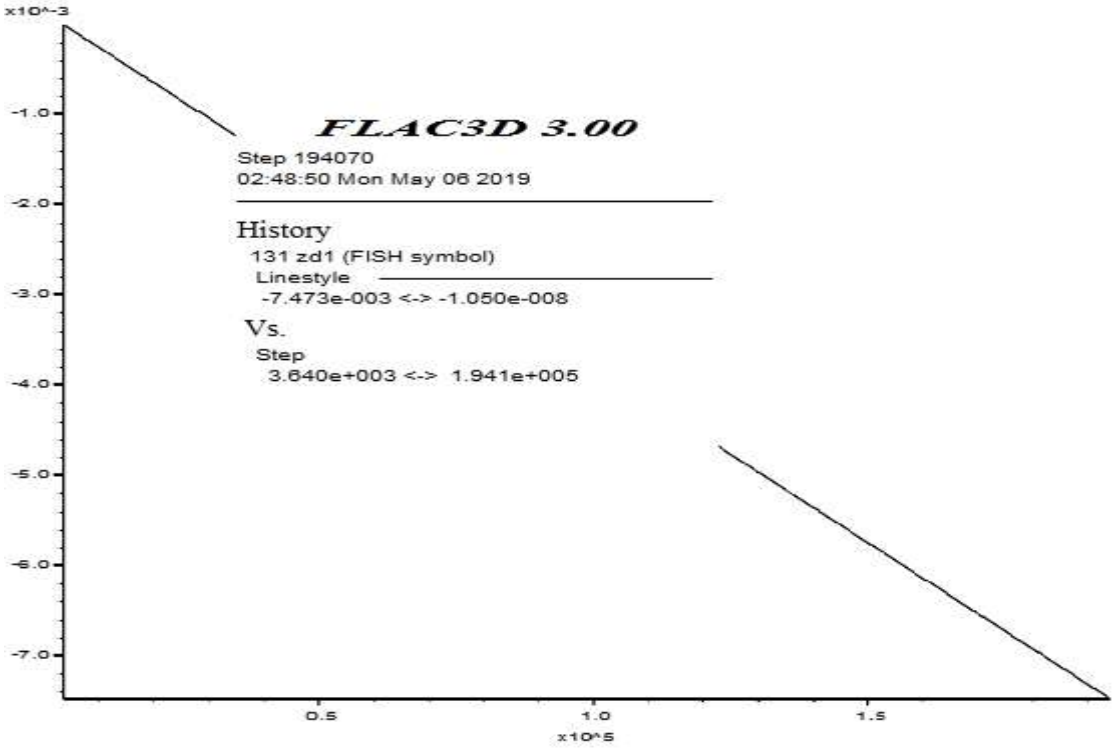

Figure B.3 Displacement of pile Head with 30 Hz vibrational loading

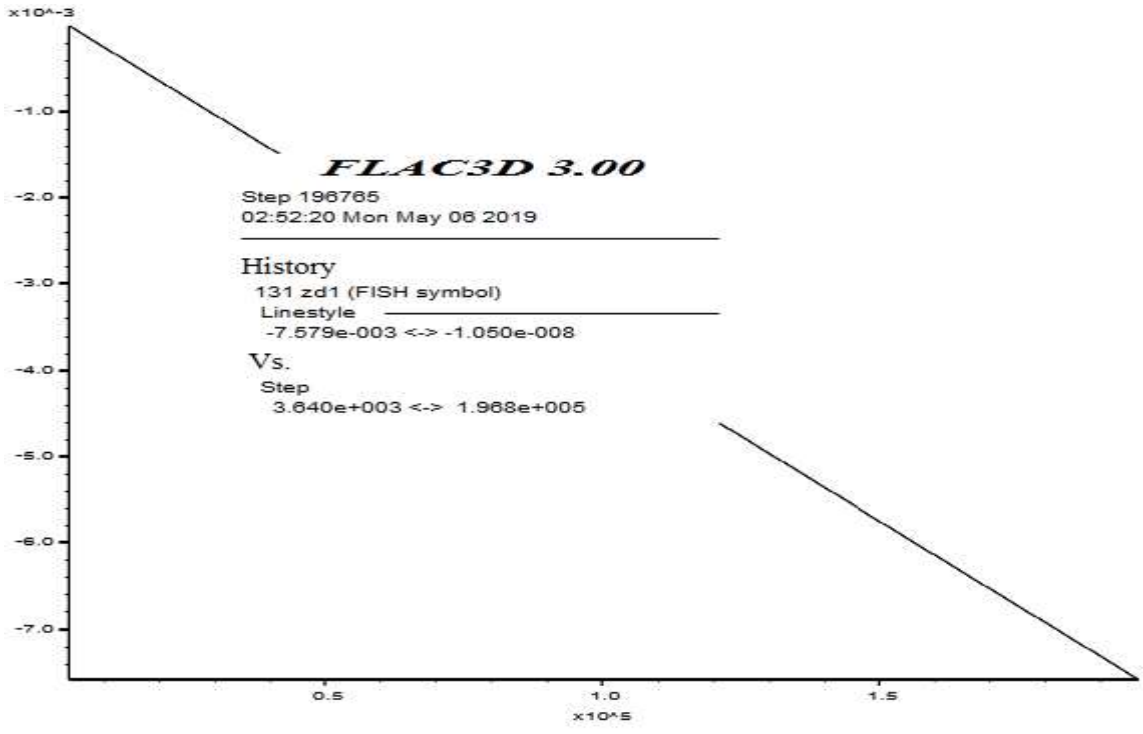

Figure B.4 Displacement of pile Head with 40 Hz vibrational loading

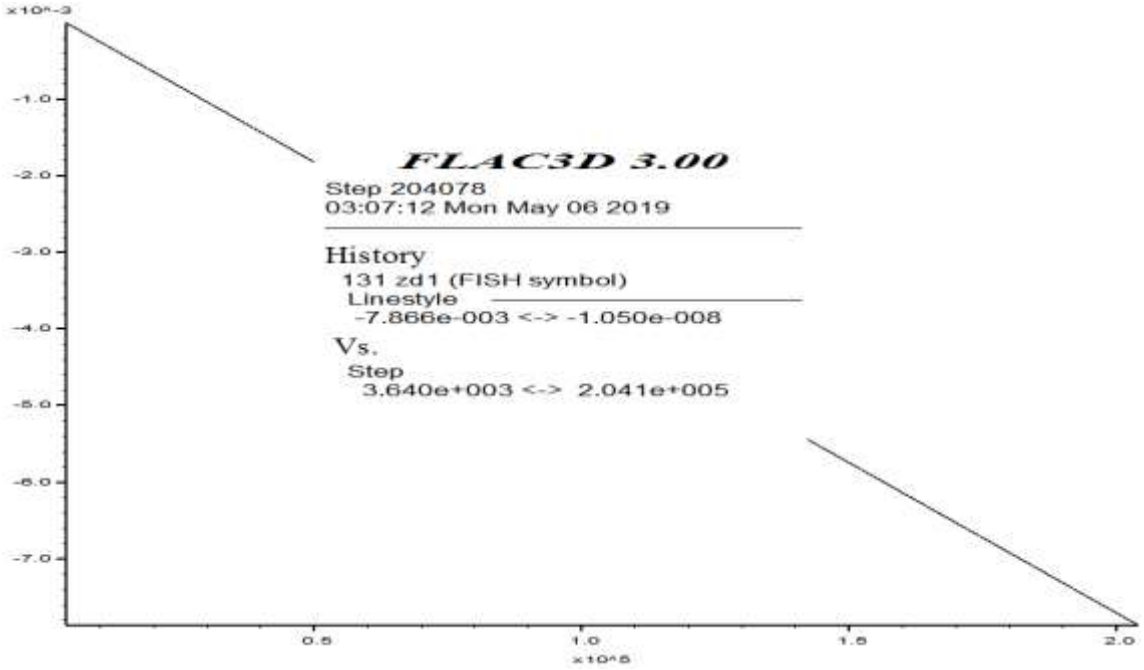

Figure B.5 Displacement of pile tip with 50 Hz vibrational loading

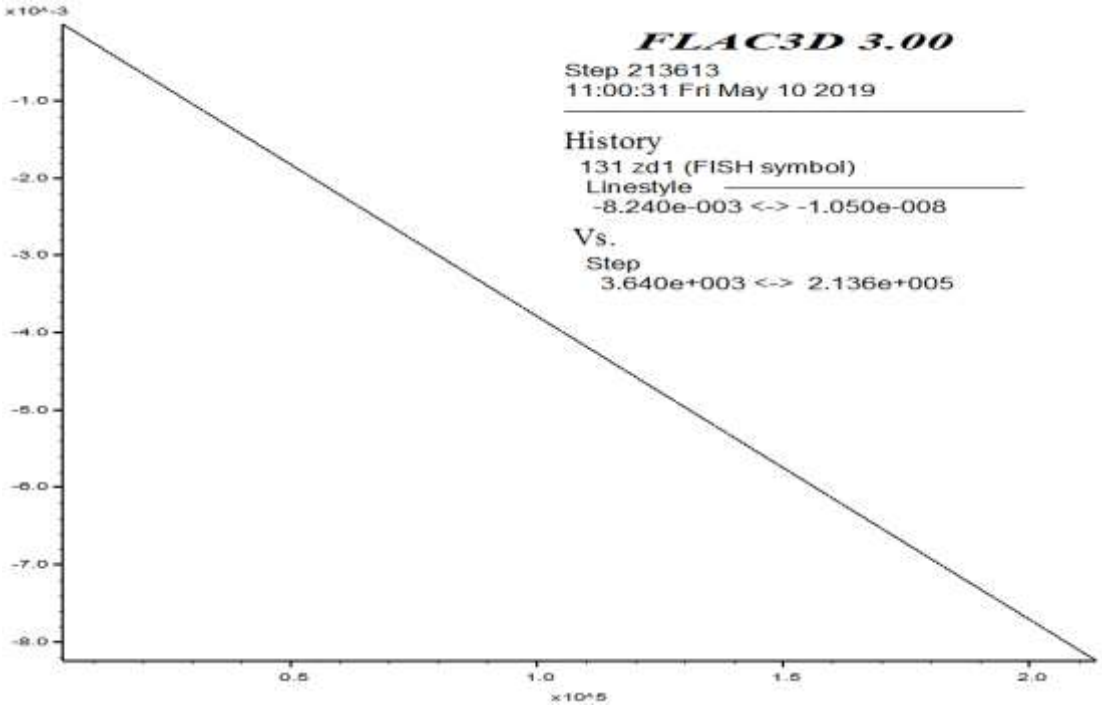

Figure B.6 Displacement of pile tip with 60 Hz vibrational loading

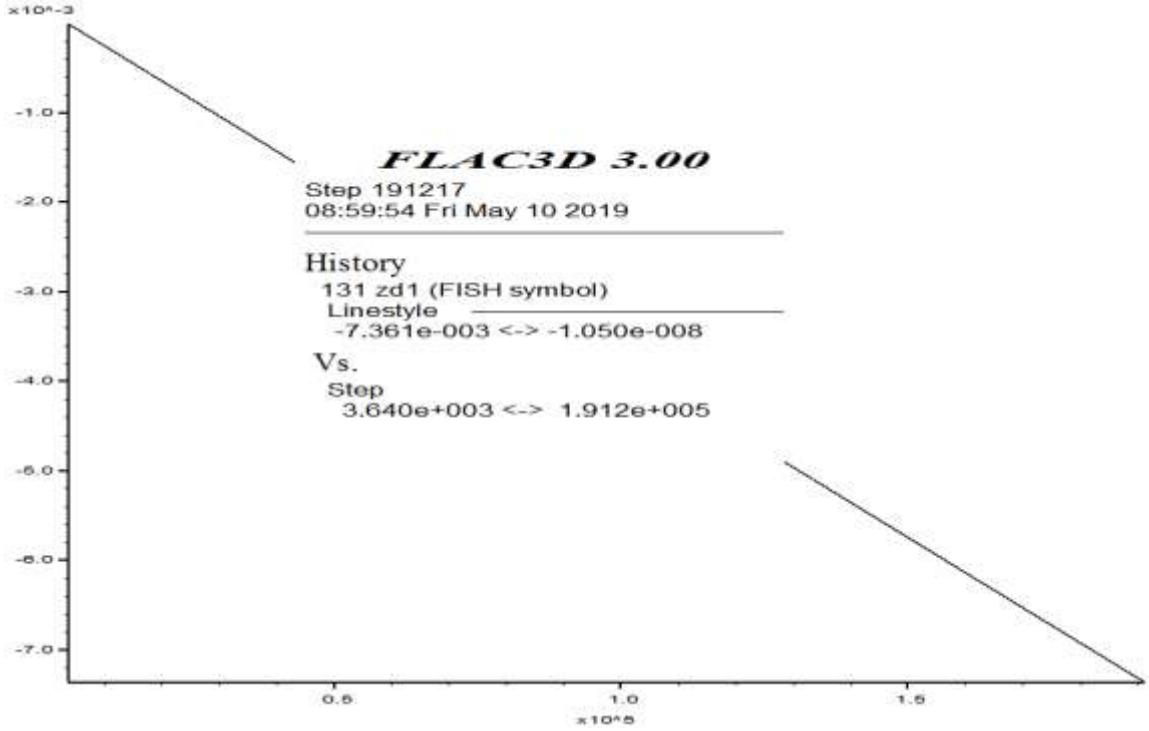

Figure B.7 Displacement of pile tip with 70 Hz vibrational loading

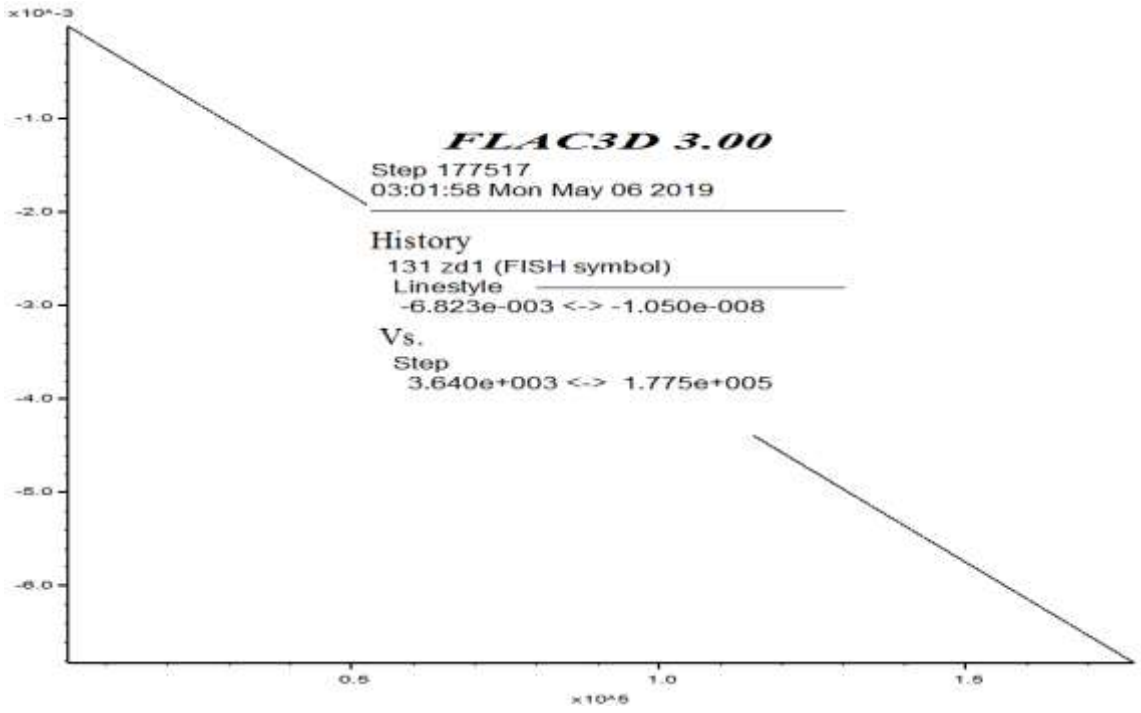

Figure B.8 Displacement of pile tip with 80 Hz vibrational loading

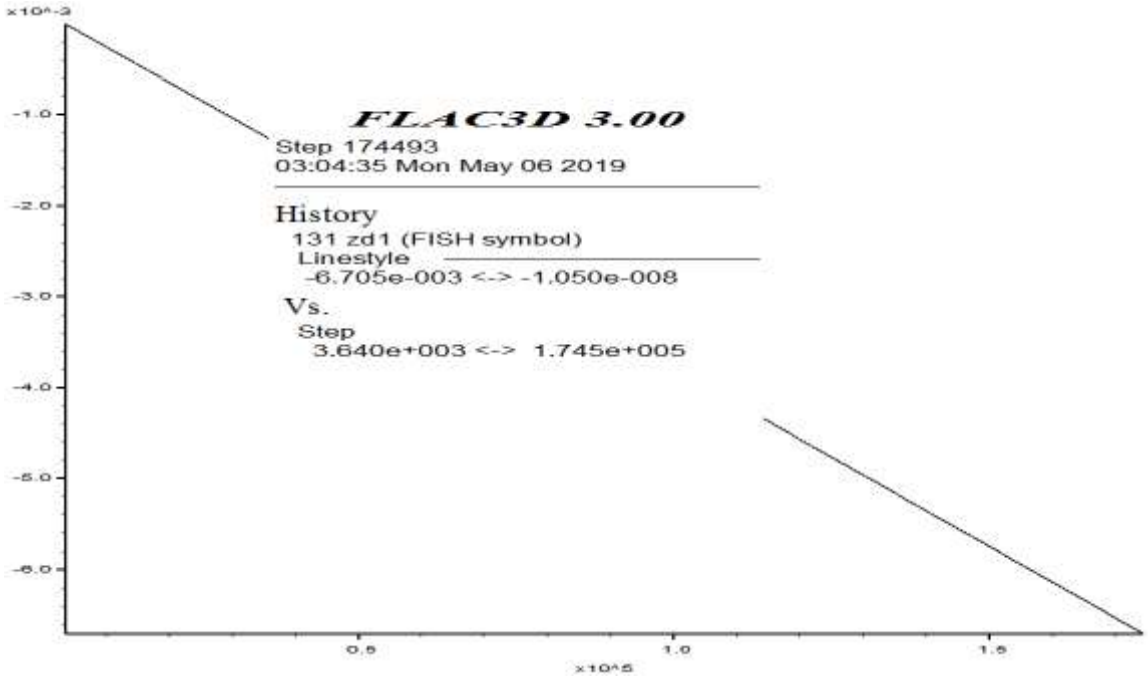

Figure B.9 Displacement of pile tip with 90 Hz vibrational loading

APPENDIX C: REPRESENTATIVE CONTOUR AT 60 HZ FREQUENCY.

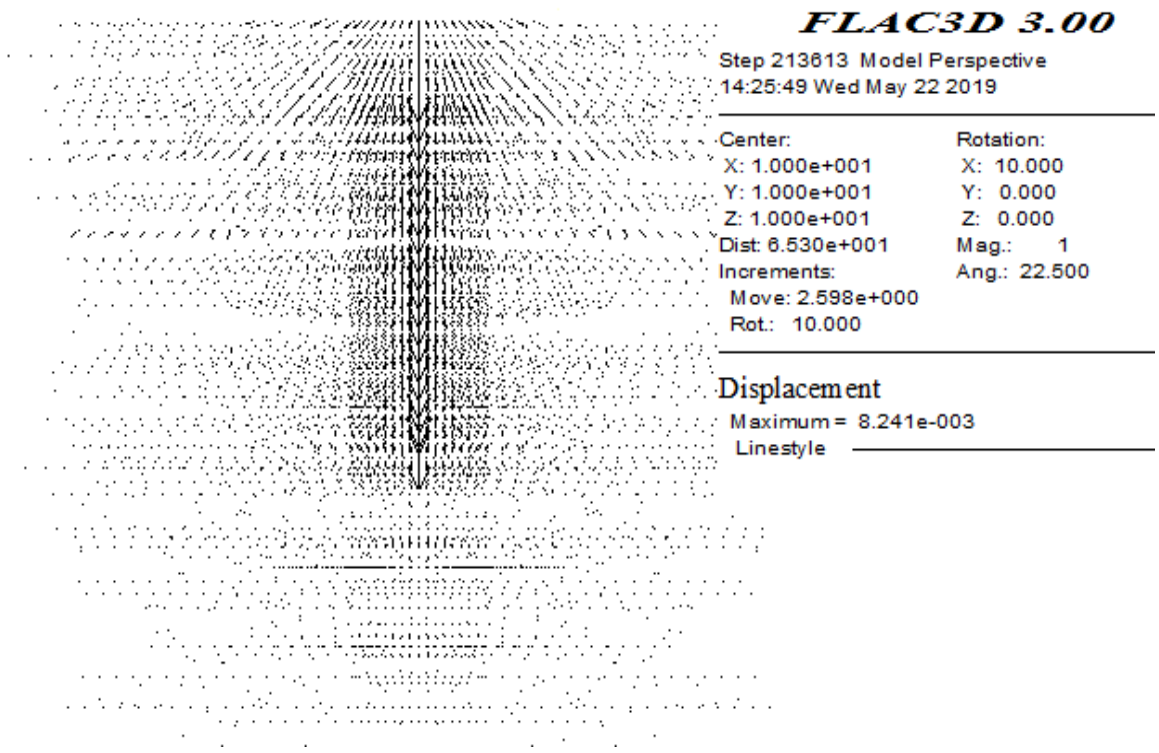

Figure C.1 Sample Resultant Displacement vector contour of frequency 60 Hz

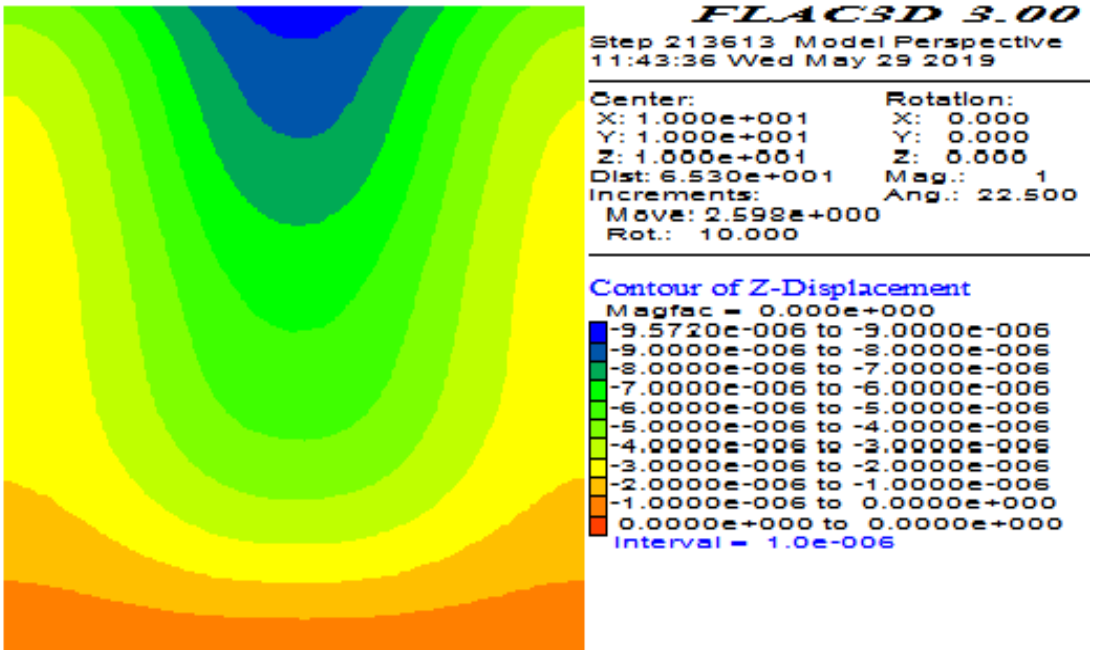

Figure C.2 Sample Z displacement contour

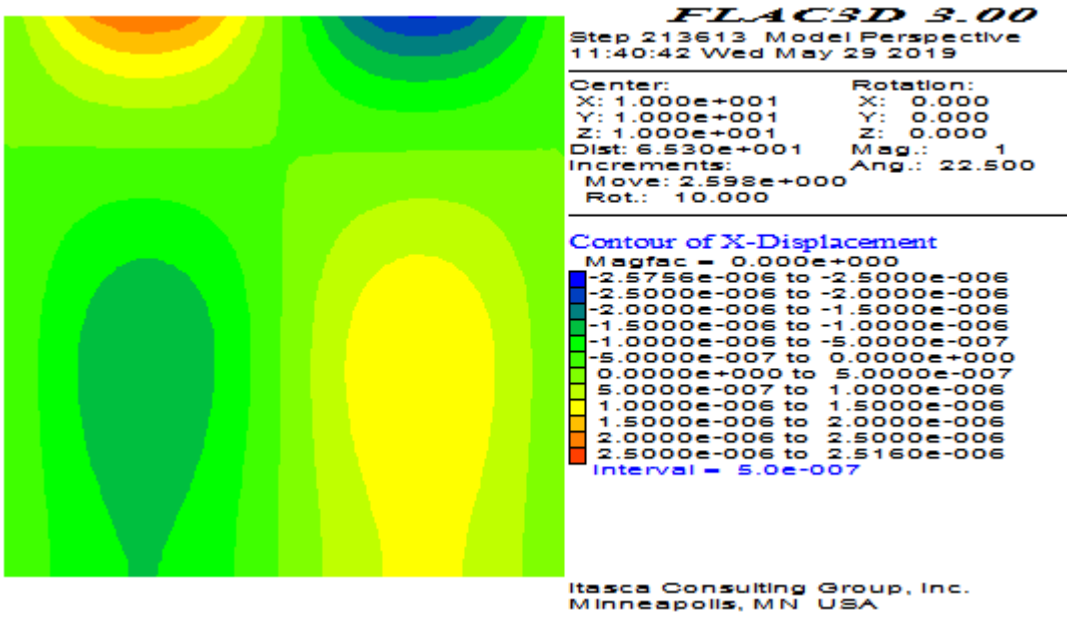

Figure C.3 Sample X displacement contour.

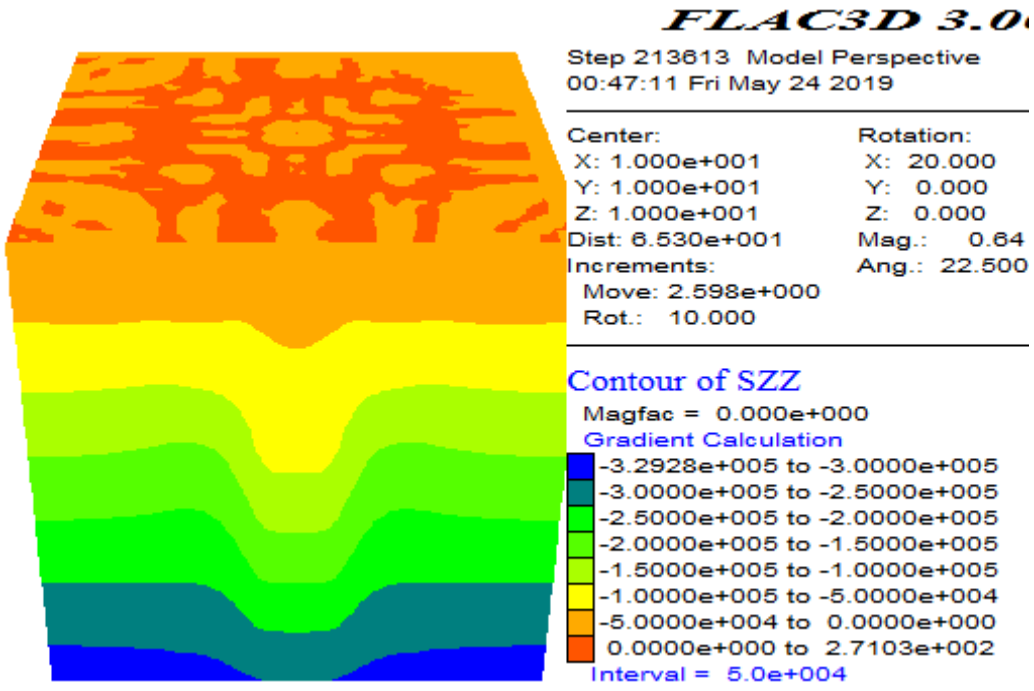

Figure C.4 Sample stress distribution contour